Building and Environment 205 (2021) 108312

Contents lists available at ScienceDirect

Building and Environment

journal homepage: www.elsevier.com/locate/buildenv

The effect of photocatalytic coatings on NO_x concentrations in real-world street canyons

E. Brattich [a,*], F. Barbano [a], B. Pulvirenti [b], F. Pilla [c], M. Bacchetti [a], S. Di Sabatino [a]

[a] Department of Physics and Astronomy "Augusto Righi", University of Bologna, via Irnerio 46, 40126, Bologna, BO, Italy
[b] Department of Industrial Engineering, University of Bologna, viale del Risorgimento, 2, 40136, Bologna, Italy
[c] Department of Planning and Environmental Policy, University College Dublin, Dublin, D14, Ireland

ARTICLE INFO

Keywords:
Air pollution
Nitrogen oxides
Photocatalytic coatings
Passive control systems
Street canyons

ABSTRACT

The abatement performance of photocatalytic coatings on NO_x concentrations in real-world street canyons remains an open question considering the very different conclusions reached by the few previous field studies. To fill this gap, an intensive experimental campaign was carried out in summer 2018 in the outskirts of Bologna in Italy. The experimental design involved two parallel street canyons in an open-air controlled environment fully instrumented for measuring air pollutant concentrations, meteorological and turbulence variables in presence of a photocatalytic coating. Specifically, the coating utilized TiO_2 photocatalysts. Several controlled pollutant release experiments with a known pollutant source were conducted within the two canyons, of which one coated with TiO_2 and the other free (reference canyon). The comparison of observations in the two canyons indicated a distinct behavior of airflows, leading to higher concentrations in the coated canyon. Three independent methods were developed to demonstrate the abatement performance of the coatings in an open-air controlled environment. The first method involved the comparison of the two canyons before and after the application of the coating; the second one regarded the derivation of normalized concentrations to remove the effect of the different geometry and dilution volume of the canyons; the third method involved dispersion modeling simulations conducted during the controlled pollutant release experiments. All the three methods demonstrated a photocatalytic reduction of NO_x in the range of 14–21%, suggesting the potential effect of photocatalysis under real weather conditions.

1. Introduction

Air pollution continues to be an important global problem with diverse and substantial health implications. The World Health Organization (WHO) currently estimates that exposure to air pollution causes 4.2 million deaths every year, 25% of which from heart diseases and 43% from lung diseases. In addition, air pollution levels remain dangerously high in many areas, with 91% of the world's population living in places where air pollution exceeds WHO guideline limits [88]. According to the 2018 Environmental Performance Index, poor air pollution is the greatest environmental threat to public health, and diseases related to airborne pollutants contributed to the 65% of all life-years lost due to environmentally related deaths and disabilities in 2016 [46].

Challenges to maintaining and improving air quality include population growth, migration toward urban areas where exposure to traffic-related pollutants tend to be higher, and growing demand for energy and transportation. In recent decades, rapid urbanization has deeply affected the environment, especially air pollution, land use, and the climate [5].

Nitrogen oxides are among the most dangerous air pollutants because these contaminants act as precursors of secondary air pollutants such as ozone, nitric acid, and secondary particulate matter [78], and because of direct and indirect effects of NO_x exposure on human health [10,80]. These include respiratory symptoms such as wheeze and cough [8,43], increase in susceptibility to respiratory infections [24], emphysema-like lesions [86], cellular damage to the throat and lungs [50] and increased mortality [57].

In general, road traffic is the most important source of NO_x emissions

* Corresponding author.
E-mail address: erika.brattich@unibo.it (E. Brattich).

https://doi.org/10.1016/j.buildenv.2021.108312
Received 7 June 2021; Received in revised form 24 August 2021; Accepted 28 August 2021
Available online 1 September 2021

in Europe, contributing to the 39% of the land-based NO_x emissions in the EU28 countries[1] [38], and is one of the main reasons why several countries frequently exceed the European annual mean limit value of 40 μg m^{-3} including Germany, France, Austria, Belgium, and Ireland [40,66,85]. The exceedance of the Europe's ambient NO_2 air quality limit is mostly attributed to emissions from diesel cars [20,33,59]. Indeed, emission measurements indicate that EURO 3, 4, 5 and 6 light-duty diesel vehicles may have higher emissions under actual driving conditions than older diesel vehicles [26]. Moreover, even though NO_x concentrations have shown a decreasing trend in emissions, NO_2 concentrations at roadside air monitoring stations have shown only small decreases, or even increases at some locations, since the mid-1980s [59,61]. This lack of reductions in roadside NO_2 concentrations has been partially attributed to the increasing proportion of primary NO_2 in the total NO_x emissions from diesel cars [18,60,74], the large dieselization process observed in Europe over the last 15 years (e.g. [17]), and the reduced effectiveness of NO_x control technologies under urban driving conditions [19,26,87]. While existing air pollution control policies and technology include measures to reduce the concentrations (g m^{-3}), emission rates (g s^{-1}) and total emissions (g) of contaminants, the direct control of air pollution concentrations in the urban atmosphere and the exposure of the population have received relatively limited attention [42,64]. Since current emission control technologies have been limited and innovative technologies may need for long time and considerable expenses to implement, passive control systems including photocatalytic coatings have been increasingly considered as solutions to mitigate air pollution without requiring enforcement, significant capital investment, or changes in human behavior [48].

Air purification through heterogeneous photocatalysis represents an emerging control option, though its application and performance during real weather conditions is still a matter of debate. In principle, among the possible semiconductors, TiO_2 in the anatase form is the most widely employed due to its strong oxidizing power under UV irradiation, its chemical stability, and its non-toxicity (e.g., [1,47,72]). In synthesis, depending on its phase (anatase, rutile or brookite), the bandgap of solid-state TiO_2 at the surface of the material (3.2 eV) enables its photoactivation when irradiated by UV-radiation with a wavelength less than 380 nm, i.e., in the UVA range [32]. Since UVA radiation emitted by the sun is not much affected by the atmosphere and reaches the surface, this characteristic enables the use of photocatalysis by TiO_2 without the need to add UV lamps [3]. Subsequently, the pollutants are oxidized due to the presence of the photocatalyst and precipitated on the surface of the material. Finally, the products of the reaction can be removed from the surface by rain and by cleaning/washing with water.

Laboratory experiments conducted to test the efficiency of photocatalytic coatings in removing NO_x pollutants indicate the potential for high reductions (e.g., [2,9,32,71,81]). The laboratory results have been confirmed by studies in artificial street canyons and in pilot scale studies, achieving NO_x reductions of 25–30% [45], and 40–80% [63,70]. However, only few field studies have been conducted in real urban street canyons and urban tunnels, reporting inconclusive and contrasting results [11]. Four of these indicated important NO_x reductions of 19% [6], higher than 30% [44], 26–66% [51], and 20% with peaks of 50% [52]. Others indicated negligible effects of the order of 2% reductions [49,55,56,82]. Also, recent studies using Computational Fluid Dynamics (CFD) simulations for representing the photocatalytic oxidation reaction are not in agreement, yielding very low values around 4% [89] and in the range 10–20% [73].

The inherent complexity in analyzing pollutant removal in real urban environments depends on the multitude of different atmospheric processes involved at different spatial and temporal scales. The circulation within the canyon is related to the local morphology of the neighborhood, building shapes and orientation. Among other factors, air circulation results from the interaction between the unperturbed background flow and the perturbations caused by the buildings' drag force and its spatial heterogeneity, and the height of the shear layer affecting the exchange of momentum between the canyon and the atmosphere above [15,35]. Flow patterns affecting dispersion within the canyon depends on the background flow conditions [25], the morphology of the canyon [14], the impact of buoyancy [29], and the presence of local gradients [27]. This complexity and the intrinsic diversity of circulation and dispersion patterns which can clearly mask the effects of photocatalytic coatings on pollutant concentrations make the analysis of the effectiveness of the coatings in real-world conditions extremely challenging and requiring a careful design of the experiment in order to examine the effects of flows and dispersion on pollutant concentrations (e.g., [31]).

This article reports the results obtained during an intensive experimental field campaign organized in the summer 2018 within the European funded iSCAPE ("Improving the Smart Control of Air Pollution in Europe") project (https://www.iscapeproject.eu/). The experimental site comprised two real street canyons within the Lazzaretto area in the outskirts of Bologna (44°29′ N, 11°20′ E, Italy). The purpose of this study was to evaluate the efficacy of TiO_2 photocatalytic coatings for NO_x abatement during weak synoptic conditions. In addition, due to its specific morphology and configuration, the Lazzaretto site represents an open-air laboratory inside a real city, much alike a controlled environment. This is the first intensive field campaign ever realized of this kind to analyze the effect of photocatalytic coatings in real environments.

To this aim, besides detailed data analysis of the high-resolution air quality and meteorological observations gathered in the two canyons, dispersion modeling simulations of the study area were also setup and conducted. After the Introduction section, this work is organized as follows: Section 2 describes the experimental design and strategy of this experimental campaign and the methods adopted to evaluate the efficacy of the coatings in reducing NO_x concentrations in real-world street canyons; Section 3 and Section 4 presents an overview of the meteorological and turbulence observations and of air pollutant concentrations observed at the experimental site, respectively; Section 5 presents the results about the efficacy of the coatings in real-world street canyons as evaluated by the three independent methods aforementioned and finally Section 6 draws the conclusions of this work.

2. Experimental design and strategy

Previous laboratory studies clearly indicate that the purifying effect of photocatalytic coatings is best exerted in closed environments where pollutant concentrations can be successively reduced by the iterative effect of the same coating unit. Based on this consideration, the street canyon can provide the perfect environment to test the coating efficacy. The reduced natural ventilation of street canyons [13,84] enables the same air mass to recursively collide with the walls of the canyon, especially in conditions of wind speed above a critical threshold and within narrow canyons [54]. For these reasons, we chose to conduct the experimental campaigns in two parallel street canyons identified in an open-air controlled environment from 4th August 2018 to 28th August 2018. This choice makes our experimental design original and more complete with respect to previous existing works conducted in pilot scale studies [63], in locations with reduced availability of UV rays like tunnels (e.g. [49,52]), or in two consecutive street canyons [6].

2.1. Experimental site

The city of Bologna is located in the southern Po Valley in northern Italy, at the foothills of the Apennines mountain chain. The Po Valley is almost entirely surrounded by the Alps and Apennines mountain chains,

[1] European Union countries: Belgium, Bulgaria, Czech Republic, Denmark, Germany, Estonia, Ireland, Spain, Greece, France, Croatia Italy, Cyprus, Latvia, Lithuania, Luxembourg, Hungary, Malta, the Netherlands, Austria, Poland, Portugal, Romania, Slovenia, Slovakia, Finland, Sweden, United Kingdom.

except for the eastern side facing the Adriatic Sea. Due to its geographical location, the Po Valley is characterized by slow wind regimes and frequent stagnant conditions (e.g., [21,58]).

The study site is the Lazzaretto area (44°30′ N, 11°19′ E), a neighborhood located within the Navile district of the Municipality of Bologna, about 3 km north-west of the Bologna city center and extending over about 3500 m^2 (Fig. 1a). The area hosts several departments of the University of Bologna, and the campus site is adjacent to a busy road linking the Bologna suburbs with the city center. This road is subjected to high traffic volumes especially during rush hours and school days. Thus, local emissions of air pollutants from traffic and residential heating in the cold season dominate the concentration levels.

The Lazzaretto area is organized as an array of buildings with similar dimension, shape and materials, and whose rooftops are gently sloping and supporting solar panels. Thus, the Lazzaretto site provides an open-air laboratory inside a real city, much alike a controlled environment with regularly shaped, equally tall buildings surrounding the street. The simplicity of the site layout allows to reproduce field investigations under real-world conditions. For the evaluation of the effectiveness of TiO_2 photocatalytic coatings in reducing the concentrations of NO_x pollutants, two parallel street canyons were identified within the Lazzaretto area as they share the same NW geographic orientation and are affected by the same emission sources (Fig. 1b). In the remainder of this paper, these canyons will be referred as canyon A and B according to Fig. 1b. The canyons presented different aspect ratios (height H equal to 8.8 and 10.8 m, width W equal to 5.3 and 12.1 m, aspect ratio H/W equal to 1.66 and 0.89, respectively for canyon A and B), and different lengths (equal to 19 and 71 m, respectively for canyon A and B) which might result in different air residence times [69] due to expected differences in air circulation and pollutant dispersion of each canyon. To characterize the air flow and turbulence and their impacts on pollutant concentrations in the canyons, a symmetrical set of high-frequency instrumentation was deployed in each canyon. Fig. 1a shows the locations of the Lazzaretto area together with air quality and meteorological stations in the city of Bologna where additional observations for this study were gathered.

2.2. Instrumental setup

To measure local pollutant concentrations two mobile laboratories (kindly provided by one of the iSCAPE partners, the Emilia-Romagna Environmental Protection Agency ARPAE) equipped for measurements of NO_x, NO, NO_2, O_3, and CO were located in each canyon. The ARPAE van located in canyon B also collected 30min average BTEX (Benzene, Toluene, Ethylbenzene, Xylene) concentrations. ARPAE mobile laboratories were also instrumented with cup anemometers and thermo-hygrometers for the measurements of wind speed, wind direction and temperature with 1min resolution. Four sonic anemometers, four temperature and humidity probes as well as two barometers were installed to measure the 3-dimensional (3-D) wind field, air temperature, air relative humidity and atmospheric pressure with high frequency, both inside and above the canyons. In-canyon instrumentations were mounted respectively at 3 m within canyon A (site A_S) and 4 m within canyon B (site B_S) above the surface, to maintain the proportion between each canyon height and the elevation of its inside instrumentation. Above-canyon instrumentations were mounted 2 m above the respective rooftop height, defining the rooftop level sites of canyon A (site A_R) and canyon B (site B_R) respectively. Sites A_R and B_R were integrated with two net radiometers to evaluate the radiative energy balance from 1-min samples. Sonic anemometers sampled at 20 Hz, thermo-hygrometers at 1 Hz, while. Gaseous air pollutants were sampled at 0.02Hz.

The meteorological station located at the "Guglielmo Marconi" airport (44°31′ N, 11°17′ E, 38 m asl) (Fig. 1a) were used to address the unperturbed background flows behavior when the station site is upwind to the city. Meteorological observations taken at ARPAE "Bologna Urbana" (44°30′ N, 11°19′ E) urban and "Asinelli" (44°29′ N, 11°20′ E, 98 m asl) synoptic meteorological stations (Fig. 1a) were instead used to downscale the synoptic conditions to local effects in order to assess the vertical structure of the atmosphere and the stability conditions necessary to discriminate local meteorological and turbulent patterns.

"Porta San Felice" (44°29′ N, 11°19′ E) and "Chiarini St." (44°29′ N, 11°17′ E) are the two closest ARPAE air quality monitoring stations respectively characterized as urban traffic and suburban background sites, providing hourly average concentrations of air pollutants NO_x, NO, NO_2, O_3, BTEX (Benzene, Toluene, Ethylbenzene, Xylene) and CO (only at "Porta San Felice"), which were used to characterize the background pollution advected to the Lazzaretto area. The technical specifications of the whole instrumentation apparatus are reported in Table 1.

After a pre-cleaning with high-pressure water and a drying of the surfaces to ensure the adhesion of the product on the original surface and not on the dirt, the walls and ground surface in one of the two canyons (Canyon A) were sprayed with PURETi TiO_2 photocatalytic coatings (PURETi coat[2]) using an electrostatic gun on 07th August 2018. The total area treated was equal to 1250 m^2 using about 12.5 l of product. The other canyon (Canyon B) was left untreated and served as a control site. Measurements taken before the coating of Canyon A were used to understand and evaluate the existing meteorological and air quality differences between the two canyons before the application of the photocatalytic coatings. Thus, the comparison of meteorological and air pollution observations in the two street canyons provided means to evaluate the effectiveness of the coatings on NO_x pollutant reduction.

2.3. Experimental protocol and quality check

Limitations in the traffic rates are due to the choice of the campaign period (summer) and to the location of the Lazzaretto area. Being a university campus, the experimental site is closed to vehicular traffic and accessible only to the allowed University staff. Moreover, the Lazzaretto campaign was carried out during the month of August, when the traffic rate is largely reduced due to the summer holiday season. Therefore, the pollutant concentrations observed within the canyons during the period were mostly associated with background concentrations transported from elsewhere, thus limiting the direct comparison between the two canyons due to their different flow residence times. To enhance the possibility of comparison and constrain the pollution source in the two canyons, a total of eight (2 nighttime on 17th August and six during daytime: one on 06th August, one on 13th August, three on 17th August, one on 18th August) controlled pollutant release experiments with a known pollution source (one EURO-2 diesel car) were organized in the two canyons. During each experiment, the car was first left idling for 20 minutes in canyon A, and then moved to canyon B where was left again idling, to minimize the difference in driving activities and cold start emissions in the two canyons. Therefore, each experiment is composed of two subsequent idling cycles of 20 minutes to release pollutants from the same source in both canyons, enabling a direct comparison of the pollutant concentrations.

Raw measurements from sonic anemometers were transformed into high-quality clean data by first eliminating all the spikes using a procedure similar to [53]. The despiking procedure assumes a Gaussian distribution inside a stationary set of data (5 minutes' interval in the data series). Values falling outside 3.5 standard deviations from the mean are rejected. Despiked wind components are then rotated to align the reference system to that of the streamline so that the wind speed U can be decomposed into its streamwise u, cross-stream v and vertical w wind components (following [65]). Once data have been despiked and rotated, both mean flow and turbulent quantities are computed at the two levels inside and above the canyons. To ensure general robustness of the analysis, without losing small-scale processes, all quantities have

[2] For a detailed description of the coatings the reader is referred to https://pureti.com/technology/faqs.html

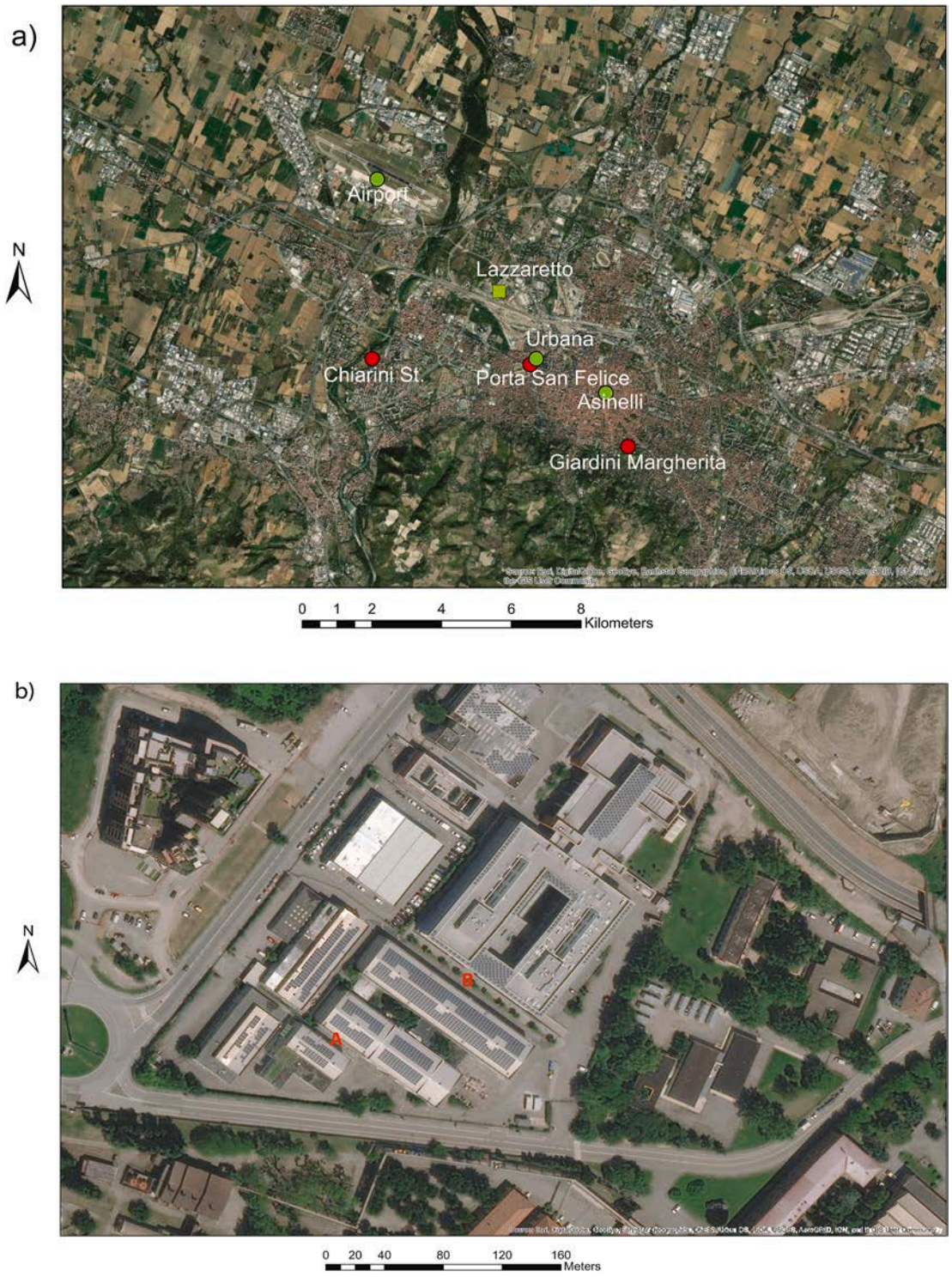

Fig. 1. a) Map of Bologna indicating the position of the Lazzaretto area (yellow square) and of other meteorological (green dots) and air quality (red dots) stations; b) Map showing the two street canyons (A = coated canyon; B = reference canyon) in Lazzaretto area in the outskirts of Bologna (Source: ESRI, DigitalGlobe, GeoEye, EarthStar Geographics, CNES/Airbus DS, USDA, USGS, AeroGRID, IGN, and the GIS User Community). (For interpretation of the references to colour in this figure legend, the reader is referred to the Web version of this article.)

been averaged to 5 minutes. Second-order turbulent quantities, such as momentum and sensible heat fluxes, were computed using the eddy-covariance technique [4].

The relative instrumental uncertainty for hourly mean NO_x concentrations was calculated following the European standard EN 14211:2012 [83] and is in the range 10–12% for both instruments used in the two canyons. All the data below the Limit of Quantification (LOQ) were discarded before data analysis (2–3% of NO_x data in the A and B canyon, respectively).

Data collected within the Lazzaretto experimental campaign were subjected to a thorough statistical analysis; statistical differences between the measurements collected in the two canyons were evaluated using pairwise Mann-Whitney test [90]. Conservatively, *p*-values in the latter were compared against adjusted significance levels α using the

Table 1
Overview of the meteorological and air pollution measurements and their time resolution in the Lazzaretto field campaign.

	GROUND LEVEL	ROOFTOP LEVEL	MODEL	SAMPLING RESOLUTION
Meteorological and turbulence variables				
SONIC ANEMOMETER	✓	✓	GILL Windmaster 3D	20 Hz
THERMO-HYGROMETER	✓	✓	HC2S3-L Campbell Scientific	1 Hz
BAROMETER	✓	✓	Vaisala PTB110	1 Hz
NET RADIOMETER	✓	✓	CNR4 Kipp & Zonen	0.02 Hz
Air pollutants				
NO_X, NO, NO_2	✓		Teledyne API Model T200 Chemiluminescence $NO/NO_2/NO_x$ Analyser	0.02 Hz
O_3	✓		Thermo Fisher Scientific Inc., Model 49i UV Photometric O_3 Analyser	0.02 Hz
CO	✓		Teledyne API T300 CO analyser	0.02 Hz
BTEX	✓ (canyon B only)		airTOXIC Chromatotech	0.0006 Hz

Dunn-Sidák correction [79] for multiple comparisons $\alpha = 1 - (1-\alpha_t)^{1/n}$, where $n = k\,(k-1)/2$ is the number of pair-wise comparisons done between k categories, with significance value $\alpha_t = 0.05$.

As mentioned before, controlled pollutant release experiments were realized to directly compare the pollutant concentrations observed in the two canyons when exposed to the same polluting source. The experiments were conducted both before and after the application of the coating in canyon A, and both during daytime and nighttime conditions, to compare the concentrations in situations with and without the activation of the coatings.

2.4. Dispersion modeling simulations

As will be shown later, the interpretation of the data acquired during the experimental campaign described previously was complemented by a series of numerical simulations of pollutant dispersion aimed to reproduce the experimental conditions and verify the effectiveness of the coatings in reducing NO_x pollutant concentrations. Specifically, to verify the expected pollutant distribution associated to a point source, the controlled pollutant release experiments realized on 17th August 2018, chosen as the one with the largest number of experiments (5 out of 8), were reproduced using the well-know and widely validated dispersion model ADMS-Urban (Atmospheric Dispersion Modeling System v4.1; [22]).

The ADMS-Urban dispersion model requires a series of minimum input data, i.e., boundary meteorological conditions (wind speed and direction, air temperature, solar radiation, cloud cover or sensible heat flux or Monin-Obukhov length for estimating boundary layer height), emission sources in the domain and background pollutant concentrations.

The simulations assumed queueing traffic moving at 5 km h^{-1} in two road sources (the closest possible condition to the car idling experiment) having the geometry of the neighborhood of the two canyons and considering the main surrounding buildings (see Supplementary Information, hereafter SI). Emission factors for this source were obtained from the national inventory of Italian road transport from ISPRA (Istituto Superiore per la Protezione e la Ricerca Ambientale), based on EMEP/EEA air pollutant emission inventory guidebook 2016 [41] and obtained with COPERT v5.1.1 software (EMISIA SA, December 2017). Emission factors were 40% increased to consider the larger emissions in idling cycles and with increasing vehicle mileage, especially affecting NO_x emissions [12]. Nighttime emissions in canyon A were further 30% enhanced to consider cold starts at lower temperatures [28].

Input values (reported in the SI as Table SI1) included hourly meteorological observations of wind speed, wind direction, air temperature, solar radiation, and cloud cover, which were obtained from the meteorological station located at Bologna airport. The 30-min average NO_x, NO_2, O_3, CO and BTEX concentrations measured in the canyon before the start of the controlled release experiments were considered as background concentrations in the simulations (reported in Table SI2). Daytime chemistry (i.e., with O_3–NO–NO_2 reactions) and dry deposition for NO_x and NO_2 gaseous pollutants were considered in the simulation. In particular, the dry deposition module of ADMS-Urban assumes a dry deposition rate proportional to the near-surface concentration as in Eq. (1):

$$F_{dry} = v_d C(x, y, 0) \tag{1}$$

where F_{dry} is the rate of dry deposition per unit area per unit time (g m^{-2} s^{-1}), $C(x,y,0)$ is the predicted airborne concentration at ground level (g m^{-3}) and v_d is the deposition velocity (m s^{-1}). As dry deposition velocity depends on the nature of the surface, the deposition velocity of NO_x pollutants here was set equal to 0.0041 m s^{-1} to consider the presence of the buildings in the simulation domain and as an average of previously reported values for NO_x [16,34] and references therein). This value is much lower than the one of 0.025 m s^{-1} obtained by a tuning of CFD model simulations setup to represent the turbulent flows and the effect of the coating on measured pollutant concentrations during the pollutant release experiments at Lazzaretto [73].

The setup of dispersion modeling simulations herein described was first validated against nighttime observed pollutant concentrations and after that compared with daytime observations to verify the presence of a further effect not considered in the numerical simulations such as the presence of the activated coatings in the canyon.

3. Meteorological and turbulence observations

In order to analyze the efficacy of the photocatalytic coating, we selected appropriate periods based on the meteorological observations and the days when the controlled-emission experiments were carried out. Specifically, we identified and compared two similar periods (one before and one after the application of the photocatalytic coatings) to assess the impact of the coatings during typical summer days. A further day is included in this analysis to evaluate the effect of the coating during the controlled pollutant emissions experiments. In the following sections, we describe the meteorological and turbulence observations during these selected periods.

3.1. The periods of weak synoptic forcing

To maximize the NO_x reduction potential of the photocatalytic coating and minimize undesired external contributions, two periods of clear-sky and weak synoptic conditions were identified to compare the same canyon before and after the application of the coating in canyon A. As the catalytic reactions in the coatings are activated by UV-solar radiation, a clear-sky condition maximizes the activation potential of the coatings. Additionally, weak synoptic conditions (when the large-scale flows have a small impact on the local circulation, leading to weak local wind speeds) enhance the possible formation of stagnant regimes within the canopy, limiting the canyon ventilation and increasing the pollutant residence time (and therefore the impact probability with a coated surface). Based on these two conditions, we selected a first period at the beginning of the campaign (04th-06th August) before the application of the photocatalytic coatings, and a second one (27th-29th August) after the application of the coating. Fig. 2 shows the incoming

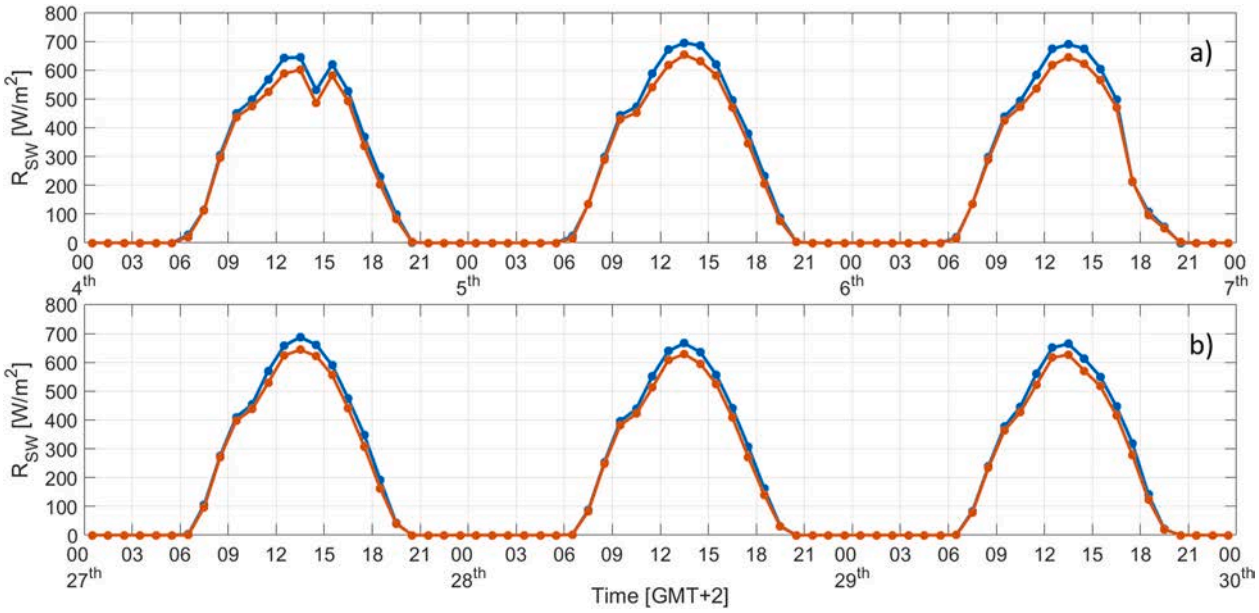

Fig. 2. 1-hour averaged incoming solar radiation R_{SW} at A_R (blue) and B_R (red) during the period 4th-6th (a) and 27th-29th (b) August 2018. (For interpretation of the references to colour in this figure legend, the reader is referred to the Web version of this article.)

shortwave radiation measured on the rooftop of the two investigated canyons during the periods before and after the coating application. A small difference (lower than 50 W m^{-2}) between A_R and B_R shortwave-radiation was observed during daytime, possibly due to an enhanced scattering component in A_R or a slightly different albedo of the rooftops. In fact, despite both rooftops are covered by a regularly shaped aluminium tinplate on top of which a patchy solar-panel array is distributed, possible differences in albedo and scattering properties may arise from the grime heterogeneously distributed on the surfaces. Nevertheless, clear-sky conditions were always detected, apart from a temporary cloud coverage observed around the 14 GMT+2 of August 4th (with no rain detected).

To assess the synoptic conditions during the periods, local air temperature and wind speed are compared with the observations from the Bologna Urbana and Asinelli Tower meteorological stations from the ARPAE permanent network. Fig. 3a (for the period 04th-06th) and Fig. 4a (for the period 27th-29th) show that the local wind speeds within and at the canyons top were typically decoupled from measurements observed at the ARPAE stations, as the large-scale flows had a small impact on the local circulation. Reduced wind speeds (with values always lower than 2 m s^{-1}) were observed within both canopies, allowing suitable conditions for the development of stagnant regimes. A wind speed decoupling was observed in canyon A between surface and rooftop measurements. This behavior depends on the morphology of canyon A, where the

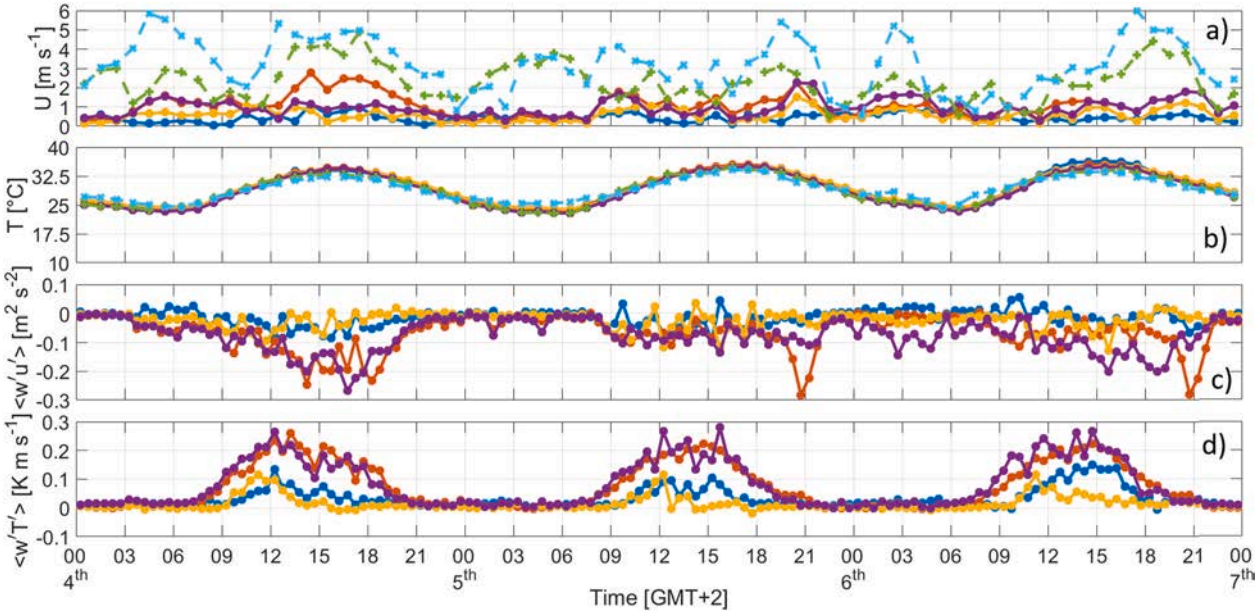

Fig. 3. 1-hour averaged wind speed (a), air temperature (b), and 30-min averaged turbulent kinematic momentum (c) and heat (d) fluxes measured in the two canyons in Lazzaretto (A_S in blue, A_R in red, B_S in yellow, B_R in purple) during the period 4th-6th August 2018. Observations of wind speed and air temperature in the two canyons are also compared with those collected at Bologna Urbana (dashed green) and Asinelli Tower (dashed cyan) meteorological stations. (For interpretation of the references to colour in this figure legend, the reader is referred to the Web version of this article.)

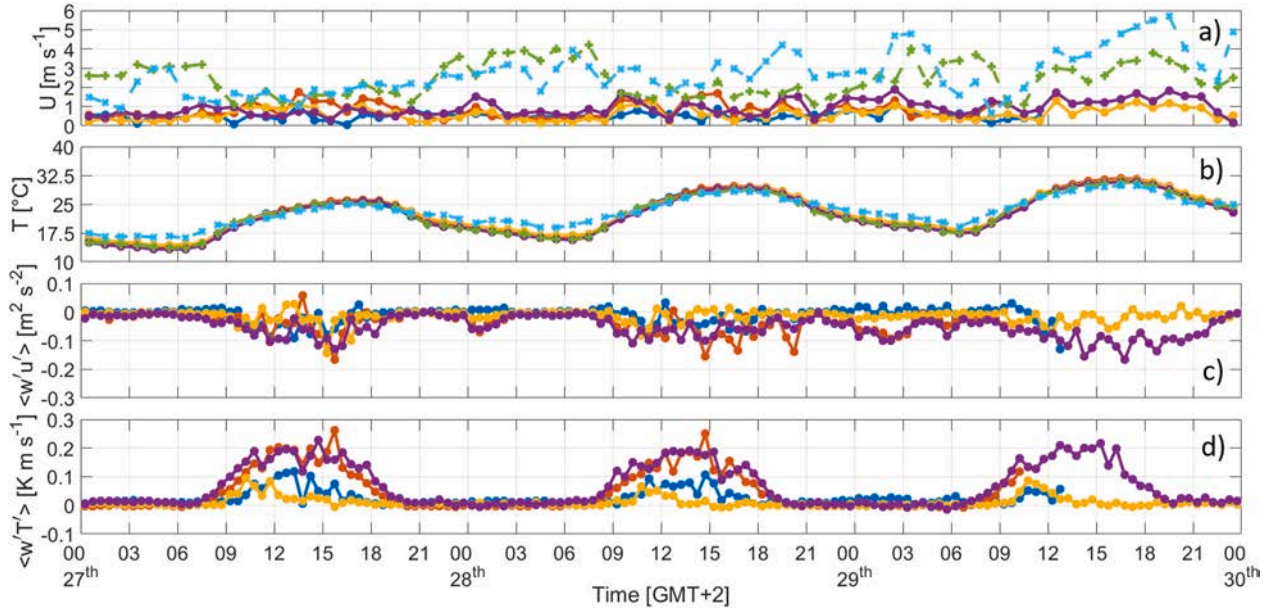

Fig. 4. 1-hour averaged wind speed (a), air temperature (b), and 30-min averaged turbulent kinematic momentum (c) and heat (d) fluxes measured in the two canyons in Lazzaretto (A_S in blue, A_R in red, B_S in yellow, B_R in purple) during the period 27th-29th August 2018. Observations of wind speed and air temperature are also compared with those collected at Bologna Urbana (dashed green) and Asinelli Tower (dashed cyan) meteorological stations. (For interpretation of the references to colour in this figure legend, the reader is referred to the Web version of this article.)

reduced canyon length enables the horizontal advection from the lateral inlet to perturb the in-canyon flow. Within canyon B, surface and rooftop wind speeds were well coupled and seemed to scale only with the dimension of the air volume allowed by the morphology.

Air temperature (Figs. 3b and 4b) shows a similar pattern during the two periods, with well-defined mixing conditions during daytime and the development of the nocturnal thermal inversion above the canopy. Even though very similar, these periods presented some differences. During the 25th and 26th August 2018 sporadic convective precipitation events were observed over the city of Bologna, temporarily modifying the pollutant concentration levels due to the enhancement of wet deposition processes. Therefore, air temperature within the second period showed increasing trends caused by the restoring adjustment to clear-sky conditions after the precipitation events. This difference might have a further impact on pollutant concentration levels, especially concerning O_3–NO_2–NO photochemical reactions, whose production-destruction rate is profoundly impacted by air temperature and solar radiation (e.g., [30]).

Due to the weak synoptic forcing and the small aspect ratios of the canyons, the skimming flow regime [67] driven by the turbulent fluxes at the rooftops is expected to characterize the local circulation, especially in canyon A where no intrusion from the mean flow has been observed. Fig. 3c and d and Fig. 4c and d shows the evolution of the turbulent kinematic heat and momentum fluxes, evaluated using the eddy-correlation technique. As expected, both momentum and heat fluxes were larger at the rooftops than inside the canyons, describing a momentum transport from the background flow to the in-canyon circulation and a larger impact of buoyancy within canyon A, where the smaller and less ventilated air volume favored the thermal mixing. In canyon B, a weak heat flux inversion can be observed during daytime in both periods, caused by the differential radiative heating of the opposite façades of the buildings.

Based on these different flow and turbulent structures in the two canyons, we can argue that the pollutant concentrations should be higher in canyon A with respect to those in canyon B, as will be described in Section 4.

3.2. The controlled-emission period

Most of the daytime and nighttime controlled-emission experiments were performed on a day (17th August) characterized by a meteorological situation almost coherent with the weak synoptic constraint presented in the previous subsection. As from Fig. 5, the levels and the pattern of incoming solar radiation were typical of the clear-sky conditions required for photocatalytic coatings activation.

The weak local wind speed constantly below 1 m s^{-1} in the coated canyon ensured the suppression of local ventilation driven by the mean flow (Fig. 6a). Mechanical ventilation generated by turbulence was also particularly weak within the canopies (Fig. 6c), where thermal mixing is expected to be significant (Fig. 6d), especially within canyon A. These low-ventilation condition enables the instauration of stagnant regimes within the canopy, favoring multiple collisions between the pollutants and the coated surfaces and thus enhancing the coating reaction probability. Not considering the upper urban boundary layer, isothermal conditions within the canyons (Fig. 6b) minimize the vertical transport caused by convective motions, further favoring stagnation. The overall low-ventilation condition was perturbed between 14:00 and 16:00 (GMT+2) by two strong turbulence events at A_S. As the nature of these perturbations is unclear, they might have a strong implication on the pollutant concentration levels within canyon A. For this reason, the interval between 14:00 and 16:00 (GMT+2) will not be used in the following analyses.

Ultimately, meteorological conditions and turbulence levels during the controlled pollutant emission period were such that the photocatalytic coatings are expected to be active and to efficiently react with the NO_x pollutants.

4. Air pollutant concentrations

In the following sections we describe the pollutant concentrations observed in the two canyons during the previously selected periods of weak synoptic forcing before and after the application of the coating, and during the controlled pollutant emission experiments.

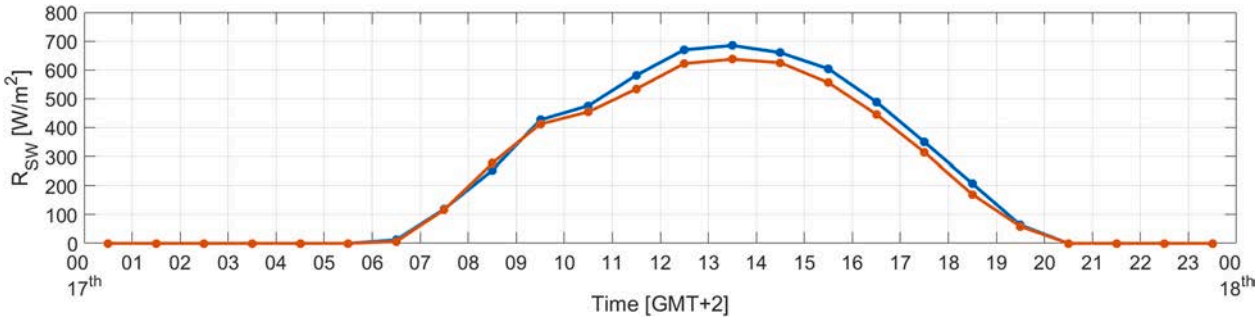

Fig. 5. 1-hour averaged incoming solar radiation R_{SW} at A_R (blue) and B_R (red) during the controlled-emission day (17th August 2018). (For interpretation of the references to colour in this figure legend, the reader is referred to the Web version of this article.)

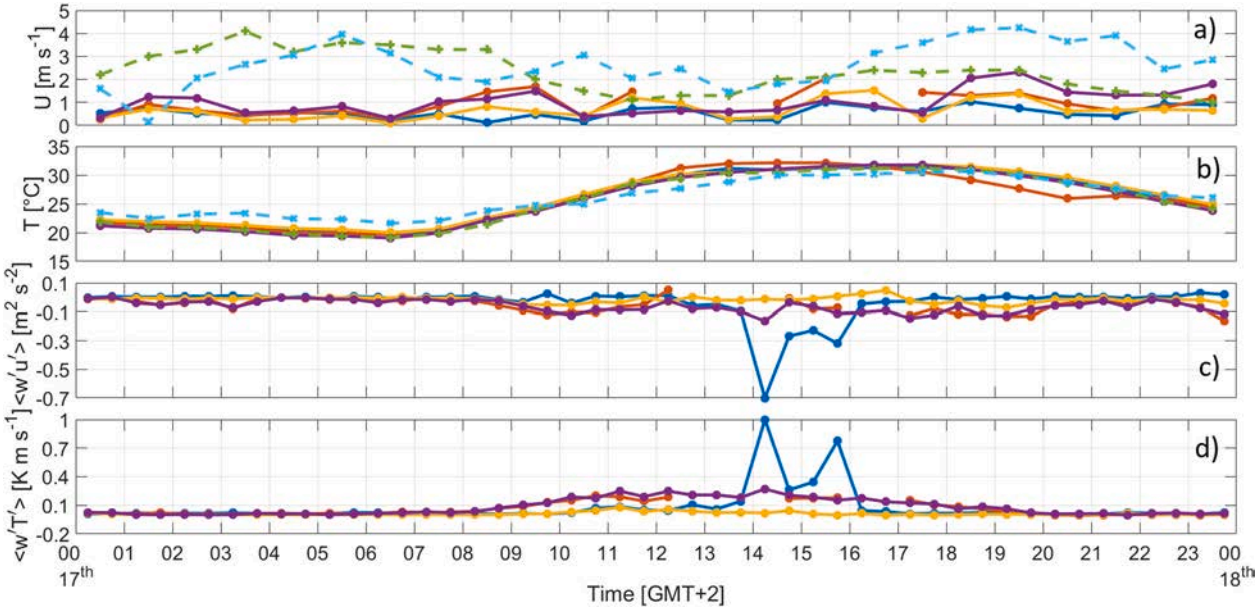

Fig. 6. 1-hour averaged wind speed (a), air temperature (b), and 30-min averaged turbulent kinematic momentum (c) and heat (d) fluxes measured in the two canyons in Lazzaretto (A_S in blue, A_R in red, B_S in yellow, B_R in purple) during the controlled-emission day (17th August 2018). Wind speed and air temperature are also compared with Bologna Urbana (dashed green) and Asinelli Tower (dashed cyan). (For interpretation of the references to colour in this figure legend, the reader is referred to the Web version of this article.)

4.1. *The two periods of weak synoptic forcing*

According to the outcomes of Section 3.1, and specifically based on these different flow and turbulent structures in the two canyons, we may suspect that the pollutant concentrations should be higher in canyon A with respect to those in canyon B. Fig. 7 shows the comparison between hourly averaged pollutant concentrations observed in the two canyons during the two previously identified periods 4th-6th and 27th-28th August (on 29th the air quality measurements already stopped). In agreement with our expectations, the comparison clearly shows that higher concentrations were observed at canyon A, both before and after the application of the coating, with two important NO_2, NO and CO spikes clearly emerging on 06th and 28th August 2018 at 09–10 and 05 GMT+2. In particular, the first spike in Fig. 7 (a,b) is associated with a controlled pollutant release experiment carried out in the two canyons. Fig. 7e shows that O_3 concentrations presented similar levels in the two canyons, as expected due to the time taken for this secondary pollutant to form and be transported. All these observations are confirmed by the descriptive statistics of hourly pollutant concentrations recorded in the two canyons during the two identified periods, as reported in Table 2. The concentrations within the two canyons were not significantly different during the two identified periods. In particular, the observation of similar O_3 concentrations and diurnal patterns (Fig. 7e) indicates that the two canyons were affected by the same background concentrations of long-distant transported secondary pollutants. Moreover, the concentration differences for the other pollutants were found to depend on local factors, such as the previously investigated coupling between the flows inside and above the canyons. This result is also confirmed by the observation of the non-significantly different NO/NO_2 ratios in the two canyons (Table 2), which suggests the influence of similar emission sources and the similar average age of air masses residing there [77]. In addition, the average high ratios in the two canyons (Table 2) suggest that both canyons were similarly distant from the main emission sources (local major roads) which means that there was enough time for the mixing with background air and conversion of NO to NO_2 [23,75].

4.2. *The controlled-emission period*

Here we present the air quality observations in the two canyons, focusing on the controlled-emission period. The boxplots in Fig. 8 present the main statistics of day and nighttime 1-min pollutant concentrations measured in the two street canyons during the 17th August 2018, focusing only on the controlled pollutant release experiments, considering not only the 20 min of the release but also the times

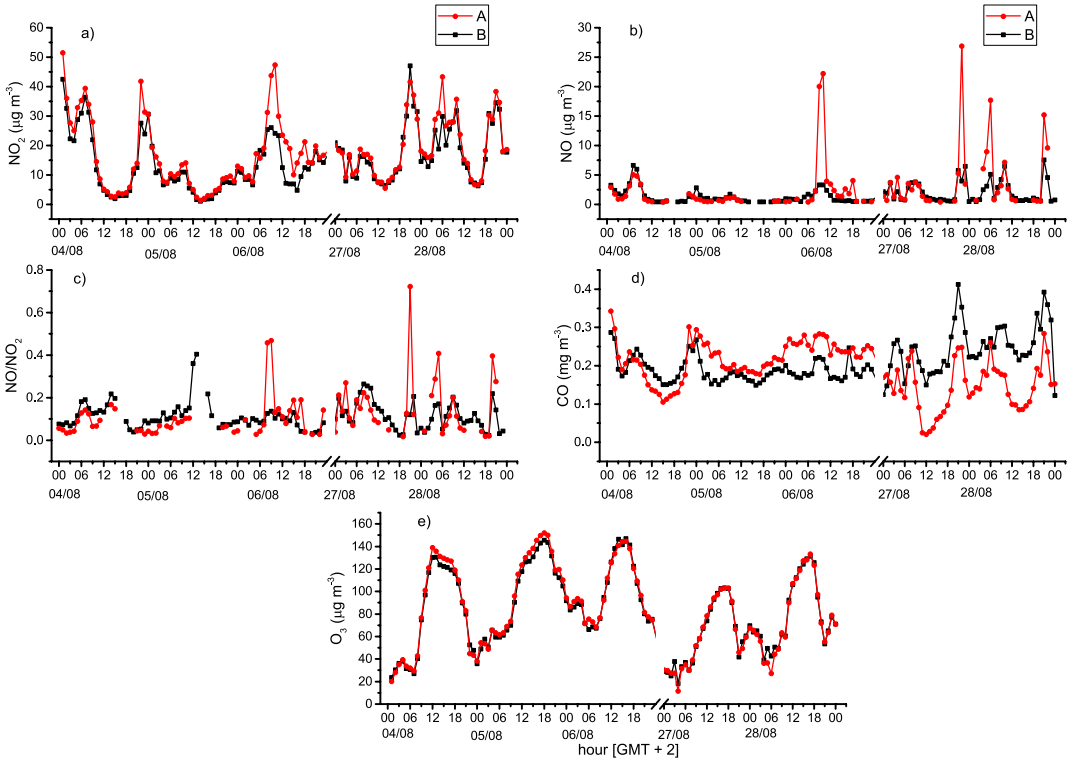

Fig. 7. Hourly pollutant concentrations (NO_2 in panel a, NO in panel b, CO in panel d, O_3 in panel e) and NO/NO_2 ratio (panel c) observed in the two canyons (red = canyon A; black = canyon B) during the two identified periods of weak synoptic forcing, before and after the application of the coatings in canyon A: 4^{th}-6^{th} (before the break in the x-axis) and 27^{th}-28^{th} (after the break in the x-axis) August 2018. (For interpretation of the references to colour in this figure legend, the reader is referred to the Web version of this article.)

Table 2
Descriptive statistics (number of cases, mean, stddev = standard deviation, min = minimum, pct25, pct50, pct75 = 25th, 50th and 75th percentile, max = maximum) and significant differences (sig diff) of hourly pollutant concentrations observed in the two canyons during the two identified periods 4th-6th and 27th-28th August 2018. For each variable, equal letters in the last column indicate the absence of significant differences (with overall significance level of 0.05).

	CANYON	CASES	MEAN	STDDEV	MIN	PCT25	PCT50	PCT75	MAX	SIG DIFF
NO_2 (μg m^{-3})	A	120	18	12	1.4	9	16	27	52	a
	B	120	15	10	1.1	7.4	12	22	47	a
NO (μg m^{-3})	A	84	3.1	4.9	0.4	0.6	1.2	3.5	27	a
	B	114	1.7	1.6	0.4	0.6	0.9	2.3	7.6	a
O_3 (μg m^{-3})	A	120	84	37	12	55	79	119	152	a
	B	120	83	35	18	57	76	113	147	a
CO (mg m^{-3})	A	120	0.19	0.07	0.02	0.1	0.2	0.2	0.3	a
	B	120	0.21	0.05	0.12	0.2	0.2	0.2	0.4	a
NO/NO_2	A	84	0.12	0.12	0.02	0.04	0.09	0.14	0.72	a
	B	114	0.11	0.06	0.02	0.07	0.10	0.14	0.40	a

immediately after (2–5 min) when the concentrations remained far higher than those measured before the experiments.

The comparison shows again higher NO_2, NO and CO concentrations in canyon A, both during day and night, but similar O_3 concentrations in the two canyons. The analysis of significant differences between the two canyons (reported together with the descriptive statistics in the SI as Table SI3) indicates the presence of significant differences in pollutant concentrations especially during daytime apart from O_3, while during night differences are smoothed down. NO/NO_2 ratios during the controlled pollutant experiments show an opposite behavior in the two canyons, with significantly higher daytime values and significantly lower nighttime values in canyon A.

Even though to a first extent all these analyses seem to indicate the reduced or even the absence of impact of the photocatalytic coatings on NO and NO_2 concentrations, the previous analysis of the differences in the in-canyon circulations has shown that the two canyons were intrinsically different because of their different geometry, apart from the possible existence of slightly different emission sources impacting on them. Therefore, the direct comparison between the pollutant concentrations observed in the two canyons is not sufficient to draw conclusions on the effectiveness of the coatings, and methodologies capable of isolating the influence of other external factors are needed to infer the real effectiveness of the coatings in the real environment.

5. Extracting the effect of photocatalytic coatings in real world conditions

With the purpose to infer the impact of coatings on NO_x

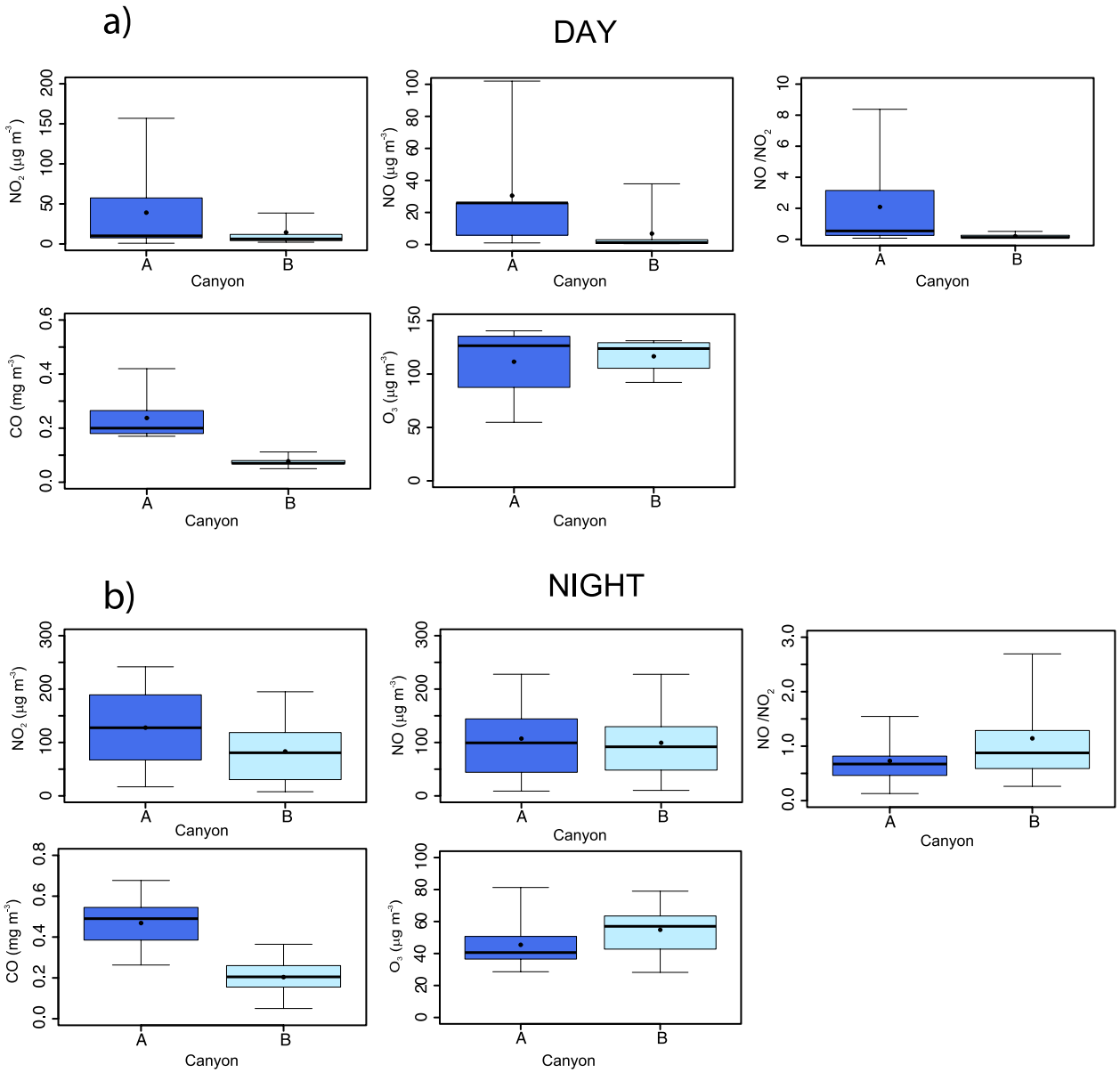

Fig. 8. Boxplots depicting the main statistical parameters for NO_2, NO, CO and O_3 pollutant concentrations and NO/NO_2 ratios observed in the two street canyons (dark blue for canyon A and light blue for canyon B) during daytime (a) and nighttime (b) 17th August 2018 controlled pollutant release experiments. The boxes enclose the 25th-75th percentile values, the whiskers represent the 5th-95th percentile values; the horizontal line inside the boxes indicates the median and the circle represents the mean value. (For interpretation of the references to colour in this figure legend, the reader is referred to the Web version of this article.)

concentrations abatement in real environments, we developed three independent methods based on totally different approaches: 1) comparison of observations in the two canyons before and after the coating of canyon A, focusing on the previously selected days of weak synoptic forcing; 2) derivation of normalized concentrations to remove the effect of the different geometry and dilution volume of the two canyons, focusing on the controlled pollutant release experiments with the purpose to minimize the effect of different emission sources impacting on the concentrations; 3) dispersion modeling simulations conducted for the coated canyon on the 17th August 2018 when most controlled pollutant release experiments were carried out.

5.1. *First method: evaluation of O_3–NO–NO_2 levels*

The first method is applied within the previously identified periods of weak synoptic conditions (4th-6th and 27th-29th August 2018) to minimize the possible differences caused by large scale airflows. Specifically, we observed that the 5th, 27th and 28th August were impacted by clear-sky conditions and similar solar radiation levels (Fig. 4). Apart from the presence of the coatings in canyon A in the two days at the end of the campaign, NO_x concentrations strongly depend on O_3 levels. Hence, we investigated the diurnal pattern of percentage ratios of O_3–NO–NO_2 (Fig. 9).

The comparison shows similar diurnal and nocturnal patterns in the two canyons considering separately each day and particularly so considering 5th and 27th August. Towards the end of the campaign, we observed a decrease in O_3 concentrations and an increase in NO_2–NO levels. This behavior might depend on the higher traffic rate in Lazzaretto area at the end of the campaign than at the beginning of the campaign, further enhanced by the fact that while 27th and 28th were working days, the 5th of August was a Sunday. In addition, the reduction in O_3 and the concurrent enhancement in NO_2 concentrations might be linked to the previously observed convective precipitation events occurred in Bologna on 25th and 26th August and the inherent reduction

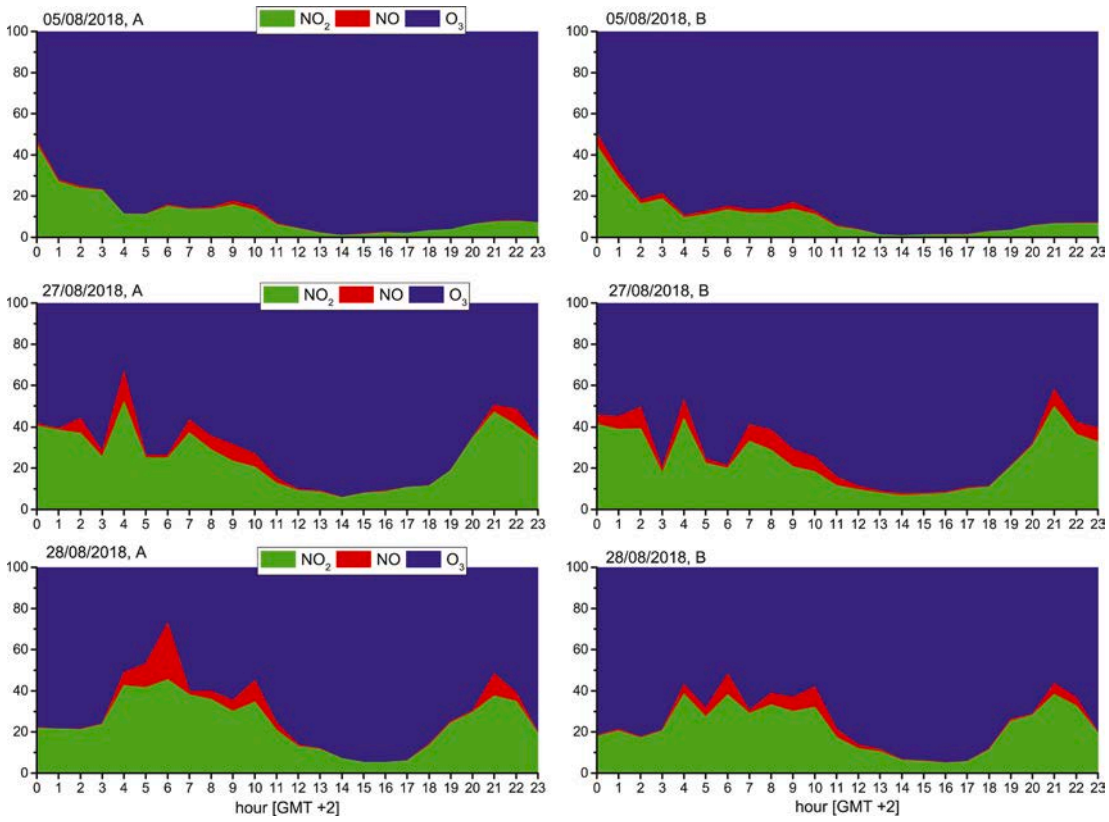

Fig. 9. Percentage ratios (in ppb) of O_3–NO–NO_2 pollutants in the two street canyons (left: canyon A; right: canyon B) in Lazzaretto area before (5th August) and after (27th and 28th August) the treatment of canyon A surfaces with photocatalytic coatings.

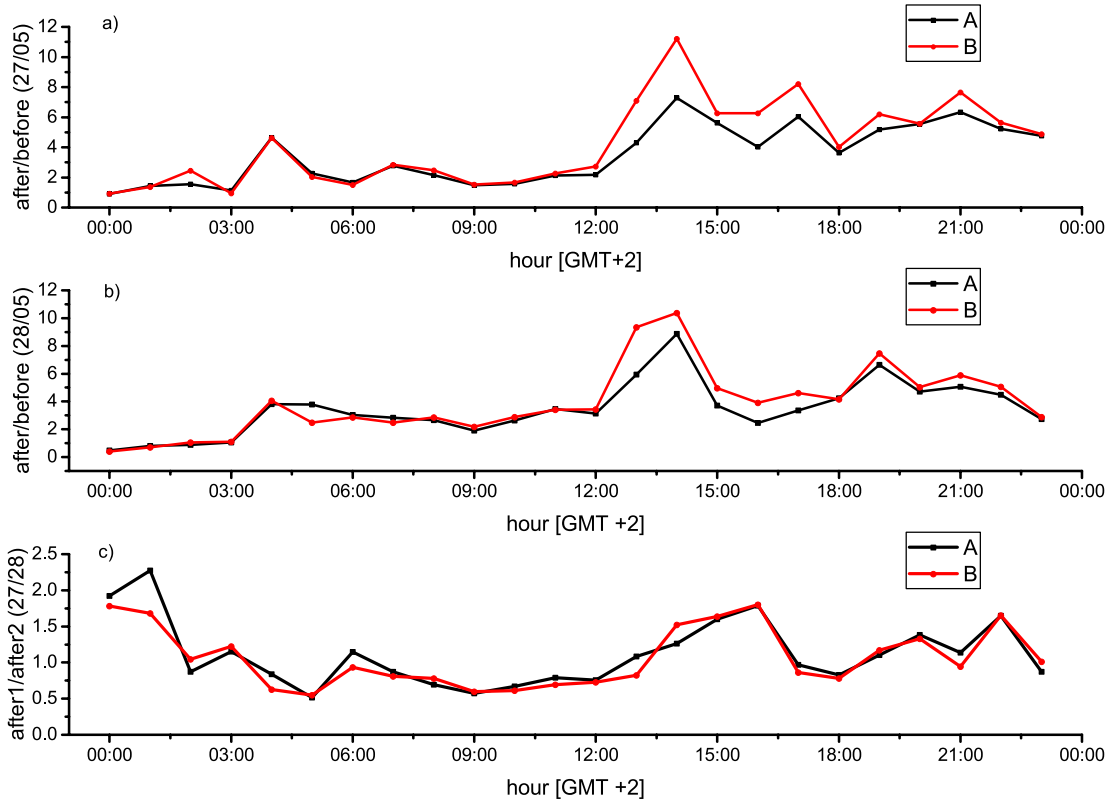

Fig. 10. Diurnal pattern of the NO_2 concentration (in ppb) ratio after/before the treatment of canyon A surfaces with photocatalytic coatings (before: 5th August; after: 27th in panel a and 28th August in panel b) and in the two days after the application of the coatings in canyon A (27th and 28th) (c), in the two canyons (black = canyon A; red = canyon B (Eq. (2)). (For interpretation of the references to colour in this figure legend, the reader is referred to the Web version of this article.)

in solar radiation and NO_2 photolysis levels, as anticipated in Section 3.1.

In order to avoid the influence of those external factors and better compare the two canyons, we calculated the ratios between NO_2 concentrations detected after (27^{th} and 28^{th} August) and before (5^{th} August) the treatment of the surfaces with photocatalytic coatings (i.e., $27^{th}/05^{th}$ and $28^{th}/05^{th}$ August, respectively) in each canyon:

$$NO_2\ rat_{A,B} = [NO_2]_{after\ A,B}/[NO_2]_{before\ A,B} \quad (2)$$

By construction, the ratio in Eq. (2) contains all the differences affecting the equilibrium reaction of O_3–NO–NO_2 simultaneously acting on the two canyons other than the photocatalytic coatings, such as the partially different meteorological conditions and the different weekdays considered in the two periods. In addition, the ratios also eliminate the different canyons geometry. Indeed, both ratios present a similar pattern in the two canyons, with lower daytime values in canyon A (Fig. 10). For the sake of completeness and to validate the method, we also calculated the ratio in Eq. (2) between the 27^{th} and 28^{th} August as a reference (Fig. 10c). It can be observed that in this case, the ratio oscillates between zero and two during the day, thus being much lower than the ratios observed when considering the days after and before the application of the coating (panels a and b), since the 27^{th} and 28^{th} August are not characterized by a difference in the activation of the coatings.

We then calculated the difference between the concentration ratios measured in the coated and in the reference canyon (A-B), normalized over the concentration ratios in the reference canyon as

$$(NO_2\ rat\ A - NO_2\ rat\ B)/\ NO_2\ rat\ B, \quad (3)$$

Once again, the differences in the NO_2 concentration ratios (shown in Fig. SI2) can be regarded as independent from the factors simultaneously affecting the NO_2–NO–O_3 equilibrium in both canyons such as the different traffic and the different meteorological conditions, while depending on the presence of the coating in canyon A only. These differences were mostly negative during daytime (06:00-18:00 GMT+2) indicating generally higher concentrations in canyon B, both considering the 27^{th} and the 28^{th} as day after the coating. On average, the daytime difference (A-B) in the NO_2 concentration ratios was equal to −15% considering the 27^{th} and −10% considering the 28^{th}, while it was significantly lower at nighttime (−4% and −1% considering 27^{th} and 28^{th}, respectively). Similar consistently low values were obtained also when considering the ratios between the two days after the application of the coatings, in this case both at daytime and at nighttime (−4% daytime, −2% nighttime) (Fig. SI2). The daytime consistent negative differences obtained only comparing the NO_2 concentrations in the two canyons before and after the application of the coatings in canyon A might be considered as a first indication of the effectiveness of the photocatalytic coatings in reducing NO_2 concentrations in street canyons at ground level. Due to the strong dependence of NO concentration on local sources and to its short lifetime and the consequent high temporal variability of this pollutant, this method was only applied to NO_2.

5.2. Second method: normalized concentrations

The second method estimates the normalized local-concentration levels in the two canyons to evaluate the photocatalytic coatings efficacy. To estimate the normalized local concentrations C^* (μg m^{-3}), we computed a factor accounting for the contribution of the urban-background concentrations within each canyon, namely the in-canyon background concentration C_b (μg m^{-3}), and subtract it from the measured concentrations C_m (μg m^{-3}) within each canyon (dividing this operation by the measured concentration in the canyon as a normalizing factor) as

$$C^*_{A,B} = \frac{C_{m_{A,B}} - C_{b_{A,B}}}{C_{m_{A,B}}} \quad (4)$$

where the subscripts A and B indicate the canyons. We focused on 4 (2 diurnal and 2 nocturnal) controlled pollutant release experiments carried out on the 17^{th} August 2018, as single occasions when the source of traffic-related pollution in the canyon can be defined as local. To estimate the in-canyon background concentration C_b, we considered all the factors potentially affecting the concentration levels in the two canyons whose contribution we want to remove, i.e., the urban background concentrations advected from long-distant sources C_0 (μg m^{-3}), the inward-outward volume flow rate $\dot{V}$ ($m^3\ s^{-1}$) in the two canyons, the residence time τ (s) of air masses in the two canyons and the dilution volume V (m^3). From a simple dimensional analysis, the in-canyon background concentrations in the two canyons were calculated as in Equation (5):

$$C_b = \frac{C_0 \dot{V} \tau}{V} \quad (5)$$

The urban background concentration C_0 was estimated as equal for both canyons from the hourly concentrations measured at Chiarini St. suburban background station the hour before the release experiment (to consider the time taken for the pollutant dispersion from the emission to the receptor); the flow rate in each of the two canyons was estimated using CFD simulations for day and night experiments [73], and its inward-outward value is the algebraic sum of the flow rate throughout each area delimiting the canyon air volume; the air residence time was estimated as the time taken for the measured concentration of CO to return to normal values after reaching its peak value. CO concentrations are chosen to compute the residence time as they are not affected by the photocatalytic coating. As such, the residence time accounts only for the pollutant removal from each canyon because of the aerodynamic effects induced by local wind and turbulence (as defined in the literature, e.g., [7,62,76]). It is important to note that none of the quantities in Eq. (5) depends on the photocatalytic-coating presence; as a consequence, the in-canyon background concentration C_b will not be dependent on the coating, leaving only C_{mA} (and C^*_A from Eq. (4)) to include the coating effects. Using Eq. (5), the normalized local concentrations for the traffic-related pollutants NO_x, NO, NO_2 (not CO since it is not measured at Chiarini suburban background station) and the controlling compound O_3 (as secondary pollutant not directly emitted by the idling car and transported from elsewhere) were then obtained within the two canyons during the release experiments.

Normalized local concentrations of O_3 (Fig. 11) were very low in both canyons during both day and night, which indicates the robustness of this method and its capacity to remove the effect of confounding factors from the concentrations observed in the two canyons. As evidenced in Fig. 11, traffic-related normalized concentrations are higher in the reference canyon (B) with respect to the coated one (A) both during day and night. Moreover, significant differences (reported in the SI, Table SI3) between daylight and nighttime experiments (evaluated using the pairwise Mann-Whitney test, see Section 2.3) are observed only in canyon A. Since all other differences between day and night (e.g., different turbulence levels) affected simultaneously both canyons, the results of this test can be considered as a further indication of the effect of the photocatalytic coatings active in canyon A during the day. In order to infer the effectiveness of the coatings with this method, we calculated the differences between the normalized local concentrations in the two canyons (B-A). These differences were on average larger during daytime, when the effect of the coatings decreases the local concentrations in A. An average concentration-reducing factor of the 14% is observed with this method during daytime, which is reduced during night and for O_3 to a 4%. This result indicates again the presence of a factor other than the different geometry and flow rates in the two canyons responsible of reducing concentrations at canyon A during daytime, in analogy with the results obtained with the first method.

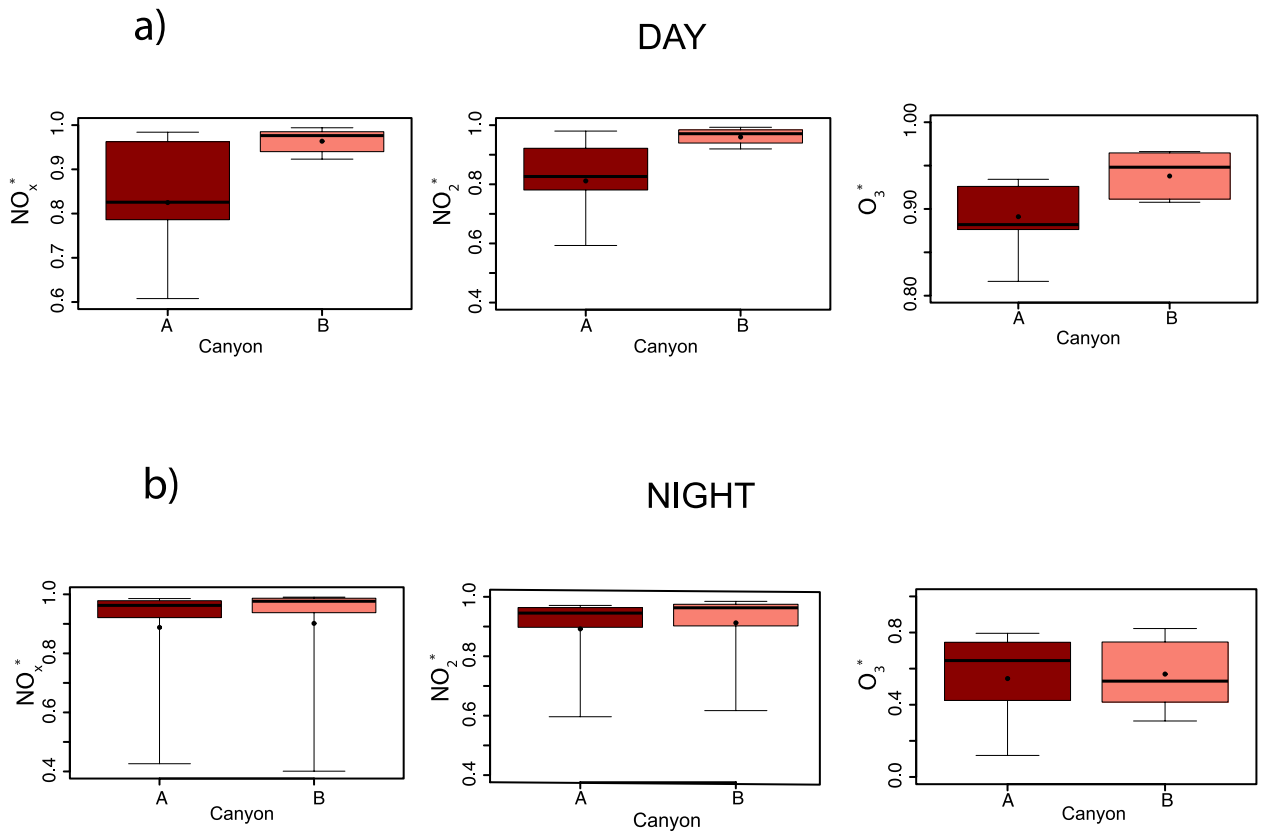

Fig. 11. Boxplots depicting the fundamental statistical parameters for normalized NO_x, NO_2, and O_3 concentrations observed within the two street canyons (canyon A in red, canyon B in salmon) in Lazzaretto area during the daytime (a) and nighttime (b) controlled pollutant release experiments. (For interpretation of the references to colour in this figure legend, the reader is referred to the Web version of this article.)

5.3. Third method: dispersion modeling simulations

The third method deals with dispersion modeling simulations of controlled pollutant release experiments conducted on the 17th August 2018 with the method drawn in Section 2.4.

Fig. 12 shows the comparison between simulated and peak average observed concentrations in canyon A.

The comparison between simulated and observed concentrations in canyon A shows good agreement for nighttime experiments (numbers 1 and 5), which serves as a validation of the model setup in correctly reproducing the emitting source. Conversely, simulated daytime concentrations tended to be higher than observations. It has to be noted here that the very low concentrations observed in canyon A during the 4th experiment seem to depend on very local meteorological factors (as previously observed from the analysis of turbulent fluxes during the period in Section 3.2) not adequately captured in these simulations, and therefore must be excluded from further discussions. However, we can observe that the simulations are able to capture the concentrations pattern, especially for NO_x. Considering the nighttime enhancement of emitting sources with respect to daytime, keeping fixed all other factors including canyon geometry and deposition velocity, it seems reasonable to suppose that the reduction in daytime observations with respect to simulated values might depend on the effect of photocatalytic coatings, not considered in the simulations. Such reduction, estimated as the difference between simulated and measured peak concentrations normalized over the measured concentrations, is in the range 8–13% for NO_2 and 15–21% for NO_x (respectively, experiment numbers 3 and 2 in Fig. 11), in good agreement with the results obtained with the two previously discussed independent methods.

5.4. Comparison of the results from the three methods

With the purpose to evaluate the ranges of the photocatalytic abatement performance retrieved, in this section we present the comparison of the results provided by the three independent methods outlined previously. Table 3 summarizes and compares the ranges of NO_2 and NO_x reduction obtained with the three independent methods described above.

The table shows that remarkably the three methods agree in indicating a reduction in NO_2 and NO_x concentrations in canyon A observable only during the day, while the nighttime reduction is limited or negligible, being the coatings activated by UV light. In addition, the three methods indicate similar and overlapping reductions of the coatings on both NO_2 and NO_x concentrations, which suggests that the potential biases by the three independent methods should be negligible. Despite the different approaches of the three independent methods, the results indicate a detectable and similar day-time reduction of NO_2 and NO_x concentrations in the coated canyon, most likely attributable to the activation of the photocatalytic coatings. Furthermore, these results are also well in agreement with those obtained with a fourth independent method based on high-resolution CFD simulations in the Lazzaretto area presented in a separate paper [73], which indicate a concentration reduction in the range 10–20%.

6. Summary and conclusions

An ad-hoc intensive field campaign was carried out within the iSCAPE H2020 project in the Lazzaretto area in the outskirts of Bologna, with the purpose of evaluating the effectiveness of photocatalytic coatings in reducing NO_x concentrations in real urban street canyons. To this aim, two parallel street canyons with the same NW orientation were

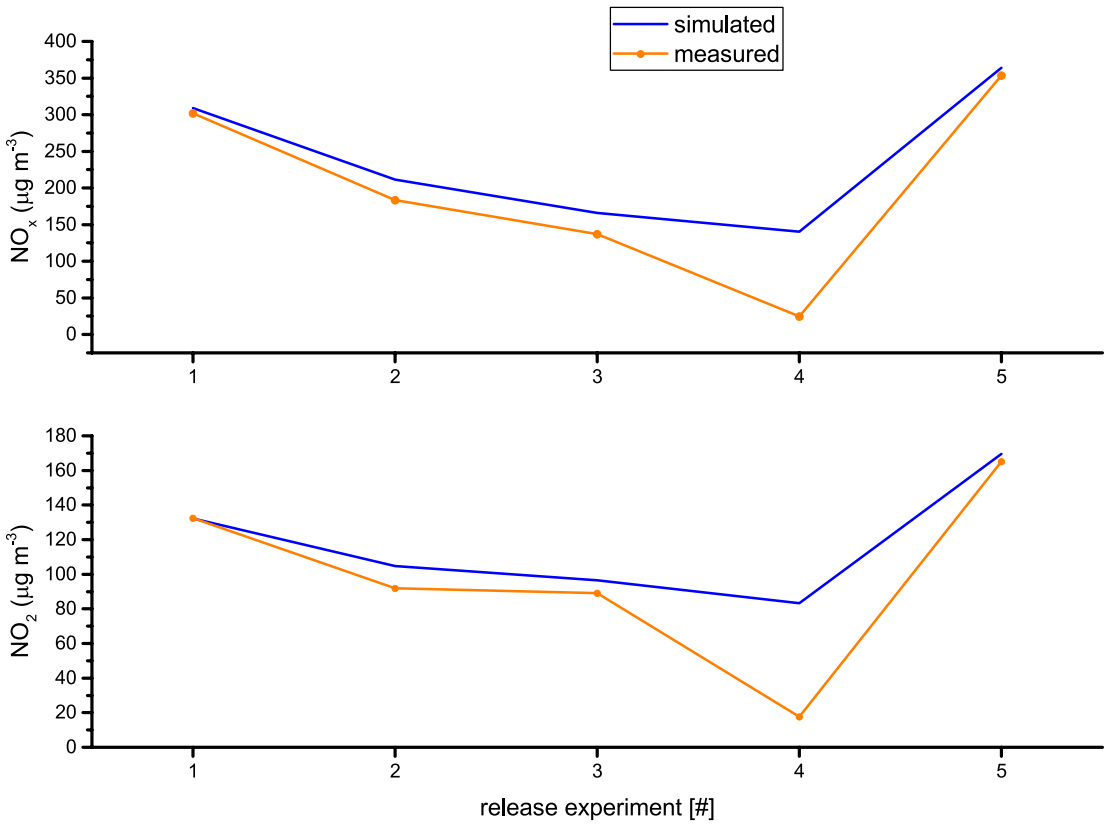

Fig. 12. Comparison of NO_2 and NO_x ADMS-Urban simulated concentrations with average peak concentrations measured in canyon A during the controlled release experiments on the 17th August. The numbers in the x-axis refer to the experiment number (1: nighttime experiment 4: 22-4:42 UTC; 2: daytime experiment 9:50-10:10 UTC; 3: daytime experiment 13:33-13:53 UTC; 4: daytime experiment 15:05-15:25 UTC; 5: nighttime experiment 20:50-21:10 UTC).

Table 3
Daytime and nighttime ranges in reduction of NO_2 and NO_x concentrations obtained with the three independent methods described above to remove the effect of confounding factors other than the coatings.

	1ST METHOD: EVALUATION OF O_3–NO–NO_2 LEVELS		2ND METHOD: NORMALIZED CONCENTRATIONS		3RD METHOD: DISPERSION MODELING SIMULATIONS	
	day	**night**	**day**	**night**	**day**	**night**
NO_2	[10, 15]%	[1, 4]%	14%	4%	[8, 13]%	[-3, −2]%
NO_X	/	/	14%	4%	[15, 21]%	[-3, 0.2]%

identified and fully equipped for flow, turbulence and concentration measurements, with several air pollutant concentrations recorded at ground level in both canyons. With the purpose to evaluate the potential of photocatalytic coatings in reducing NO_x concentrations, after a short period used to compare intrinsic differences in airflow and dispersion characteristics between the two canyons at the beginning of the campaign, one of the two canyons (canyon A) was coated, while the other was left untreated (canyon B). During the campaign, semi-controlled pollutant release experiments were conducted to directly compare the pollutant concentrations in the two canyons when exposed to the same pollutant source. Both canyons were similarly equipped for the measurements of high frequency meteorological and turbulence at two vertical levels, one inside and one above the canyons.

Two periods of weak synoptic forcing dominated by thermal circulation and similar clear sky conditions and solar radiation levels were identified at the beginning (before the treatment with photocatalytic coatings) and at the end (after the treatment with photocatalytic coatings) of the campaign. The comparison between the two canyons in those periods showed that because of their different aspect ratios the flows behave differently: in fact, while in canyon A which is characterized by a reduced length, the flow is decoupled from the rooftop, in canyon B the flows are well coupled. In addition, the small size of canyon A causes the prevalence of stagnation regimes, while canyon B presented dominant reduced thermal stratification and enhanced mixing processes.

Because of their different characteristics, a direct comparison between the concentrations observed in the two canyons, showing a general tendency for concentrations to be larger in canyon A, cannot be used to infer the effect of photocatalytic coatings. To this aim, we developed three independent methods to remove the effect of other confounding factors such as the effect of the different geometry and dilution volume before comparing the concentrations. In particular, one method consisted in a detailed analysis and in the derivation of NO_2 and NO_x concentration ratios between two meteorologically similar periods after and before the application of the coatings on the walls of canyon A but characterized by similar radiation levels and therefore similar potential activation of the coatings. The comparison between the ratios after/before observed in the two canyons, while by construction removed the factors simultaneously affecting the two canyons such as the different meteorological conditions of the two periods, indicated higher daytime concentration ratios in canyon B, therefore suggesting the effect of factors reducing NO_x concentrations active in canyon A in the second period only, such as the coatings itself. The other two methods focused on the controlled pollutant release experiments, which were used to derive normalized concentrations removing the effect of the different geometry and different flow via the calculation of background concentrations depending, besides that from pollutant concentrations advected to the study area, on the canyon's volume, the residence time of the air masses and the flow velocity in the two canyons. Even this method indicated higher concentrations in canyon B after removing the effect of other confounding factors. The third method involved the analysis of the

outputs of adequately setup dispersion modeling simulations in the coated canyon during the controlled pollutant release experiments carried on 17th August 2018. The simulations, though correctly reproducing the nighttime observations, i.e., when the coatings are not activated, indicated higher concentrations during daylight, possibly resulting from the coatings which was not reproduced in the simulations. Interestingly, all the three methods agree well indicating a daytime reduction of the concentrations in canyon A, yielding a preliminary reduction in NO_x concentrations in the range 14–21% (8–15% for NO_2).

While our analyses suggest a potential effect of the coatings in reducing NO_x (NO_2) concentrations in real street canyons, in agreement with some of the previous field studies conducted in real street canyons, considering the instrumental uncertainty which falls roughly in the middle of this range, further observations would be needed to conclude on the final impact of photocatalytic coatings in an urban environment. In particular, further analyses aimed at a better understanding of turbulent exchange processes would be necessary to better constrain the different behaviors of the two canyons: to this aim, the investigation of turbulent fluxes of carbon dioxide and water vapor, also measured within the campaign but not objective of the current study, might be very helpful to further corroborate our results.

7. Data availability

A description of the observational data and model outputs used in this paper is provided in Section 2. Observations used in this work are available as open access data on the AMS Acta online repository (http://doi.org/10.6092/unibo/amsacta/6281).

Declaration of competing interest

The authors declare that they have no known competing financial interests or personal relationships that could have appeared to influence the work reported in this paper.

Acknowledgements

This work has received funding from the iSCAPE project funded by the European Union's H2020 Research and Innovation programme (H2020-SC5-04-2015) funded under the Grant agreement No. 689954. The authors acknowledge the funding received from the iSCAPE project. This paper reflects the authors' view. The European Commission is not liable for any use that may be made of the information contained therein. The authors would also like to thank: Roberto Carli and the staff of the Department of Civil, Chemical, Environmental and Materials Engineering, the ARPAE Regional Environmental Protection Agency and the Emilia-Romagna Region in the persons of Luca Torreggiani, Carla Barbieri, Marco Deserti, Arianna Trentini and Vanes Poluzzi for the realization of the experimental field campaign at Lazzaretto campus of the University of Bologna; PURETi staff for treating the walls and ground surfaces of the street canyon in Lazzaretto with photocatalytic coatings; Richard Baldauf from the US-EPA for his valuable comments and suggestions which overall greatly improved the quality of our work; Martina Polito for her support in the realization of the field campaign; Francesca Di Nicola from the Department of Physics and Astronomy "Augusto Righi" of the University of Bologna for her support in the setup of the ADMS-Urban simulations; OpenStreet Map and contributors for providing the maps; ISPRA national institute for providing the national road transport emission factors.

Appendix A. Supplementary data

Supplementary data to this article can be found online at https://doi.org/10.1016/j.buildenv.2021.108312.

References

[1] A.G. Agrios, P. Pichat, An overview of the state of the art and perspectives on materials and applications of photocatalysis over TiO_2, J. Appl. Electrochem. 35 (2005) 655–663, https://doi.org/10.1007/s10800-005-1627-6.
[2] C.H. Ao, S.C. Lee, C.L. Mak, Y.L. Chan, Photodegradation of VOCs and NO for indoor purification using TiO_2: promotion versus inhibition effect of NO, Appl. Catal. B Environ. 42 (2003) 112–129, https://doi.org/10.1016/S0926-3373(02)00219-9.
[3] B.A. Atzl, M. Pupp, M. Rupprich, The use of photocatalysis and titanium dioxide on diesel exhaust fumes for NOx reduction, Sustainability 10 (2018) 4031, https://doi.org/10.3390/su10114031.
[4] M. Aubinet, T. Vesala, D. Papale, Eddy Covariance: a Practical Guide to Measurement and Data Analysis, Springer Science & Business Media, 2012, ISBN 978-94-007-2350-4.
[5] X. Bai, T. McPhearson, H. Cleugh, H. Nagendra, X. Tong, T. Zhu, Y.-G. Zhu, Linking urbanization and the environment: conceptual and empirical advances, Annu. Rev. Environ. Resour. 42 (2017) 215–240, https://doi.org/10.1146/annurev-environ-102016-061128.
[6] M.M. Ballari, H.J.H. Brouwers, Full scale demonstration of air-purifying pavement, J. Hazard Mater. 254–255 (2013) 406–414, https://doi.org/10.1016/j.hazmat.2013.02.012.
[7] F. Barbano, E. Brattich, S. Di Sabatino, Characteristic scales for turbulent exchange processes in a real urban canopy, Boundary-Layer Meteorol. 178 (2021) 119–142, https://doi.org/10.1007/s10546-020-00554-5.
[8] M.A. Bauer, M.J. Utell, P.E. Morrow, et al., Inhalation of 0.30 ppm nitrogen dioxide potentiates exercise-induced bronchospasm in asthmatics, Am. Rev. Respir. Dis. 134 (1986) 1203–1208, https://doi.org/10.1164/arrd.1986.134.5.1203.
[9] D.M. Blake, Bibliography of Work on the Heterogeneous Photocatalytic Removal of Hazardous Compounds from Water and Air, National Renewable Energy Laboratory, Golden, Colorado, 2001 available at, https://www.nrel.gov/docs/fy02osti/31319.pdf. (Accessed 22 July 2020).
[10] B. Boningari, P.G. Smirniotis, Impact of nitrogen oxides on the environment and human health: Mn-based materials for the NOx abatement, Current Opinion in Chemical Engineering 13 (2016) 133–141, https://doi.org/10.1016/j.coche.2016.09.004.
[11] E. Boonen, A. Beeldens, Photocatalytic roads: from lab tests to real scale applications, European Transport Research Review 5 (2013) 79–89, https://doi.org/10.1007/s12544-012-0085-6.
[12] J. Borken-Kleefeld, Y. Chen, New emission deterioration rates for gasoline cars – results from long term measurements, Atmos. Environ. 101 (2015) 58–64, https://doi.org/10.1016/j.atmosenv.2014.11.013.
[13] R. Buccolieri, M. Sandberg, S. Di Sabatino, City breathability and its link to pollutant concentration distribution within urban-like geometries, Atmos. Environ. 44 (2010) 1894–1903, https://doi.org/10.1016/j.atmosenv2010.02.022.
[14] R. Buccolieri, P. Salizzoni, L. Soulhac, V. Garbero, S. Di Sabatino, The breathability of compact cities, Urban Climate 13 (2015) 73–95, https://doi.org/10.1016/j.uclim.2015.06.002.
[15] R. Buccolieri, M. Sandberg, H. Wigo, S. Di Sabatino, The drag force distribution within regular arrays of cubes and its relation to cross ventilation – theoretical and experimental analyses, J. Wind Eng. Ind. Aerod. 189 (2019) 91–103, https://doi.org/10.1016/j.jweia.2019.03.022.
[16] California Air Resources Board, Mathematical modeling and control of the dry deposition flux of nitrogen-containing air pollutants, Final report Contract No. A6-188-32, available online at: https://ww2.arb.ca.gov/sites/default/files/classic//research/apr/past/a6-188-32.pdf, 1990. (Accessed 22 July 2021).
[17] M. Cames, E. Helmers, Critical evaluation of the European diesel car boom-global comparison, environmental effects and various national strategies, Environ. Sci. Eur. 25 (2013) 15, https://doi.org/10.1186/2190-4715-25-15.
[18] D.C. Carslaw, Evidence of an increasing NO_2/NO_x emissions ratio from road traffic emissions, Atmos. Environ. 39 (2005) 4793–4802, https://doi.org/10.1016/j.atmosenv.2005.06.023.
[19] D.C. Carslaw, S.D. Beevers, J.E. Tate, E.J. Westmoreland, M.L. Williams, Recent evidence concerning higher NOx emissions from passenger cars and light duty vehicles, Atmos. Environ. 45 (2011) 7053–7063, https://doi.org/10.1016/j.atmosenv.2011.09.063.
[20] D. Carslaw, T. Murrells, J. Andersson, M. Keenan, Have vehicle emissions of primary NO_2 peaked? Faraday Discuss 189 (2016) 439–454, https://doi.org/10.1039/c5fd00162e.
[21] S. Caserini, P. Giani, C. Cacciamani, S. Ozgen, G. Lonati, Influence of climate change on the frequency of daytime temperature inversions and stagnation events in the Po Valley: historical trend and future projections, Atmos. Res. 184 (2016) 15–23, https://doi.org/10.1016/j.atmosres.2016.09.018.
[22] CERC (Cambridge Environmental Research Consultants), Urban Air Quality Management System Version 4.1. ADMS-Urban Urban Air Quality Management System User Guide Version 4.1.1, 2017.
[23] A.M. Chaney, D.J. Cryer, E.J. Nicholl, P.W. Seakins, NO and NO(2) interconversion downwind of two different line sources in suburban environments, Atmos. Environ. 45 (2011) 5863–5871, https://doi.org/10.1016/j.atmosenv.2011.06.070.
[24] A.J. Chauhan, M.T. Krishna, A.J. Frew, S.T. Holgate, Exposure to nitrogen dioxide (NO2) and respiratory disease risk, Rev. Environ. Health 13 (1–2) (1998) 73–90, https://doi.org/10.1016/S0140-6736(03)13582-9.
[25] Z.H. Chen, S.Y. Cheng, J.B. Li, X.R. Guo, W.H. Wang, D.S. Chen, Relationship between atmospheric pollution processes and synoptic pressure patterns in northern China, Atmos. Environ. 42 (24) (2008) 6078–6087, https://doi.org/10.1016/j.atmosenv.2008.03.043.

[26] Y. Chen, J. Borken-Kleefeld, Real-driving emissions from cars and light commercial vehicles-Results from 13 years remote sensing at Zurich/CH, Atmos. Environ. 62 (2014) 657–665, https://doi.org/10.1016/j.atmosenv.2014.01.040.

[27] W.C. Cheng, C.H. Liu, D.Y.C. Leung, On the correlation of air and pollutant exchange for street canyons in combined wind-buoyancy-driven flow, Atmos. Environ. 43 (24) (2009) 3682–3690, https://doi.org/10.1016/j.atmos.env.2009.04.054.

[28] D. Choi, M. Beardsley, D. Brzezinski, J. Koupal, J. Warila, MOVES sensitivity analysis: the impacts of temperature and humidity on emissions, in: 19th Int Emiss Invent Conf San Ant Tex S6, 2010, p. P1.

[29] C. Cintolesi, F. Barbano, S. Di Sabatino, Large-eddy simulation analyses of heated urban canyon facades, Energies 14 (11) (2021) 3078, https://doi.org/10.3390/en14113078.

[30] J. Coates, K.A. Mar, N. Ojha, T.M. Butler, The influence of temperature on ozone production under varying NOx conditions-a modelling study, Atmos. Chem. Phys. 16 (2016) 11601–11615, https://doi.org/10.5194/acp-16-11601-2016.

[31] J.M. Cordero, R. Hingorani, E. Jimenez-Relinque, M. Grande, F. Cutillas, E. Martinez, R. Borge, A. Narros, A. Castellote, Challenges in quantification of photocatalytic NO2 abatement effectiveness under real world exposure conditions illustrated by a case study, Sci. Total Environ. 766 (2020) 144393, https://doi.org/10.1016/j.scitotenv.2020.144393.

[32] J.S. Dalton, P.A. Janes, N.G. Jones, J.A. Nicholson, K.R. Hallam, G.C. Allen, Photocatalytic oxidation of NOx gases using TiO2: a surface spectroscopic approach, Environ. Pollut. 120 (2002) 415–422, https://doi.org/10.1016/S0269-7491(02)00107-0.

[33] B. Degraeuwe, P. Thunis, A. Clappier, M. Weiss, W. Lefebvre, S. Janssen, S. Vranckx, Impact of passenger car NO_x emissions and NO_2 fractions on urban NO_2 pollution-scenario analysis for the city of Antwerp, Belgium, Atmos. Environ. 126 (2016) 218–224, https://doi.org/10.1016/j.atmosenv.2015.11.042.

[34] A.C. Delany, T.D. Davies, Dry deposition of NOx to grass in rural East Anglia, Atmos. Environ. 17 (1983) 1391–1394, https://doi.org/10.1016/0004-6981(83)90414-6.

[35] S. Di Sabatino, E. Solazzo, P. Paradisi, R.E. Britter, A simple model for spatially-averaged wind profiles within and above an urban canopy, Boundary-Layer Meterol 127 (2008) 131–151.

[38] EEA (European Environment Agency), Air Quality in Europe – 2018 Report, 2018 available at: https://www.eea.europa.eu/publications/air-quality-in-europe-2018. (Accessed 22 July 2021).

[40] EMEP, Emissions for 2013, Transboundary Particulate Matter, Photo-Oxidants, Acidifying and Eutrophying Components. EMEP/MSC-W Status Report 1/2015, The Norwegian Meteorological Institute, Oslo, 2015. ISSN: 1504-6109. Available online at: https://emep.int/publ/reports/2015/EMEP_Status_Report_1_2015.pdf. (Accessed 24 August 2021).

[41] EMEP/EEA, EMEP/EEA Air Pollutant Emission Inventory Guidebook 2016. Technical Guidance to Prepare National Emission Inventories, 2016. EEA report No. 21/2016. ISSN 1977-8449. Available online at: https://www.eea.Europa.eu/publications/emep-eea-guidebook-2016. (Accessed 22 July 2021).

[42] J. Fenger, Urban air quality, Atmos. Environ. 33 (29) (1999) 4877–4900, https://doi.org/10.1016/S1352-2310(99)00290-3.

[43] L.J. Folinsbee, Does nitrogen dioxide exposure increase airways responsiveness? Toxicol. Ind. Health 8 (5) (1992) 273–283, https://doi.org/10.1177/074823379200800505.

[44] A. Folli, M. Strøm, T.P. Madsen, T. Henriksen, J. Lang, J. Emenius, T. Klevebrant, Å. Nilsson, Field study of air purifying paving elements containing TiO_2, Atmos. Environ. 107 (2015) 44–51, https://doi.org/10.1016/j.atmosenv.2015.02.025.

[45] Fraunhofer, Paving slabs that clean the air, Available at, https://www.fraunhofer.de/content/dam/zv/en/documents/rn8_AUGUST_tcm63-59839.pdf, 2010. (Accessed 22 July 2021).

[46] M.J. Friedrich, Air pollution is greatest environmental threat to health, J. Am. Med. Assoc. 319 (11) (2018) 1085, https://doi.org/10.1001/jama.2018.2366.

[47] A. Fujishima, K. Hashimoto, T. Watanabe, TiO_2 Photocatalysis: Fundamentals and Applications, BKC, Inc., Tokyo, 1999.

[48] J. Gallagher, L.W. Gill, A. McNabola, The passive control of air pollution exposure in Dublin, Ireland: a combined measurement and modelling case study, Sci. Total Environ. 458–460 (2013) 331–343, https://doi.org/10.1016/j.scitotenv.2013.03.079.

[49] M. Gallus, R. Ciuraru, F. Mothes, V. Akylas, F. Barmpas, et al., Photocatalytic abatement results from a model street canyon, Environ. Sci. Pollut. Control Ser. (2015), https://doi.org/10.1007/s11356-015-4926-4.

[50] F.D. Gilliland, R. McConnell, J. Peters, H. Gong Jr., A theoretical basis for investigating ambient air pollution and children's respiratory health, Environ. Health Perspect. 107 (suppl 3) (1999) 403–407, https://doi.org/10.1289/ehp.99107s3403.

[51] G.L. Guerrini, E. Peccati, Photocatalytic Cementitious Roads for Depollution, International RILEM Symposium on Photocatalysis, Environment and Construction Materials, Florence, 2007, pp. 179–186.

[52] G.L. Guerrini, Photocatalytic performances in a city tunnel in Rome: NOx monitoring results, Construct. Build. Mater. 27 (2012) 165–175, https://doi.org/10.1016/j.conbuildmat.2011.07.065.

[53] J. Hejstrup, A statistical data screening procedure, Meas. Sci. Technol. 4 (1993) 153–157, https://doi.org/10.1088/0957-0233/4/2/003.

[54] L.H. Hu, R. Huo, D. Yang, Large eddy simulation of fire-induced buoyancy driven plume dispersion in an urban street canyon under perpendicular wind flow, J. Hazard Mater. 166 (1) (2009) 294–406, https://doi.org/10.1016/j.jhazmat.2008.11.105.

[55] IPL, Dutch Air Quality Innovation Programme Concluded, 2010. https://laqm.defra.gov.uk/documents/Dutch_Air_Quality_Innovation_Programme.pdf. (Accessed 22 July 2021).

[56] S. Jacobi, NO2-Reduzierung durch photocatalysis wirk same Oberflächen? Modellversuch Fulda, Hessisches Landesamt für Umwelt und Geologie, 2010. https://www.hlnug.de/fileadmin/dokumente/das_hlug/jahresbericht/2012/jb2012_059-066_I2_Jacobi_final.pdf. (Accessed 22 July 2021). Accessed.

[57] M. Jerrett, R.T. Burnett, B.S. Beckerman, M.C. Turner, D. Krewski, G. Thurston, et al., Spatial analysis of air pollution and mortality in California, Am. J. Respir. Crit. Care Med. 188 (5) (2013), https://doi.org/10.1164/rccm.201303.0609OC.

[58] J. Kaiser, G.M. Wolfe, B. Bohn, S. Broch, H. Fuchs, L.N. Ganzeveld, S. Gomm, R. Häseler, A. Hofzumahaus, F. Holland, J. Jäager, X. Li, I. Lohse, K. Lu, A.S. H. Prévot, F. Rohrer, R. Wegener, R. Wolf, T.F. Mentel, A. Kiendler-Scharr, A. Wahner, F.N. Keutsch, Evidence for an unidentified non-photochemical ground-level source of formaldehyde in the Po Valley with potential implications for ozone production, Atmos. Chem. Phys. 15 (2015) 1289–1298, https://doi.org/10.5194/acp-15-1289-2015.

[59] G. Kiesewetter, J. Borken-Kleefeld, W. Schöpp, C. Heyes, P. Thunis, B. Bessagnet, E. Terrenoire, A. Gsella, M. Amann, Modelling NO_2 concentrations at the street level in the GAINS integrated assessment model: projections under current legislation, Atmos. Chem. Phys. 14 (2014) 813–829, https://doi.org/10.5194/acp-14-813-2014.

[60] M. Kousoulidos, L. Ntziachristos, G. Mellios, Z. Samaras, Road-transport emission projections to 2020 in European urban environments, Atmos. Environ. 42 (2008) 7465–7475, https://doi.org/10.1016/j.atmosenv.2008.06.002.

[61] R. Kurtenbach, J. Kleffmann, A. Niedojadlo, P. Wiesen, Primary NO2 emissions and their impact on air quality in traffic environments in Germany, Environ. Sci. Eur. 24 (21) (2012), https://doi.org/10.1186/2190-4715-24-21.

[62] K.W. Lo, K. Ngan, Characterizing ventilation and exposure in street canyons using Lagrangian particles, Journal of Applied Meteorology and Climatology 56 (5) (2017) 1177–1194, https://doi.org/10.1175/JAMC-D-16-0168.1.

[63] T. Maggos, A. Plassais, J.G. Bartzis, C. Vasilakos, N. Moussiopoulos, L. Bonafous, Photocatalytic degradation of NOx in a pilot street canyon configuration using TiO2-mortar panels, Environ. Monit. Assess. 136 (2008) 35–44, https://doi.org/10.1007/s10661-007-9722-2.

[64] H. Mayer, Air pollution in cities, Atmos. Environ. 33 (24) (1999) 4029–4037, https://doi.org/10.1016/S1352-2310(99)00144-2.

[65] R. McMillen, An eddy correlation technique with extended applicability to non-simple terrain, Boundary-Layer Meteorol. 43 (3) (1988) 231–245, https://doi.org/10.1007/BF00128405.

[66] A. Minkos, U. Dauert, S. Feigenspan, S. Kessinger, Luftqualität 2016, available at: https://www.umweltbundesamt.de/publikationen/luftqualitaet-2016, 2017. (Accessed 22 July 2021).

[67] T. Oke, in: Boundary Layer Climates, second ed., Routledge, Taylor & Francis Group, 1987, ISBN 0415043190, p. 464.

[69] I. Ossanlis, P. Barmpas, N. Moussiopoulos, The effect of the street canyon length on the street scale flow field and air quality: a numerical study, in: C. Borrego, A. L. Norman (Eds.), Air Pollution Modeling and its Application XVII, Springer, Boston, MA, 2007, ISBN 978-0-387-68854-1, https://doi.org/10.1007/978-0-387-68854-1_67.

[70] PICADA, European PICADA Project, GROWTH Project GRD1-2001-40449, 2006.

[71] P. Pichat, J. Disdier, C. Hoang-Van, D. Mas, G. Goutailler, C. Gaysse, Purification/deodorization of indoor air and gaseous effluents by TiO_2 photocatalysis, Catal. Today 63 (2000) 363–369, https://doi.org/10.1016/S0920-5861(00)00480-6.

[72] P. Pichat, Photocatalytic degradation of pollutants in water and air. Basic concepts and applications, in: M.A. Tarr (Ed.), Chemical Degradation Methods for Wastes and Pollutants: Environmental and Industrial Applications, Marcel Dekker, New York, 2003, pp. 77–119.

[73] B. Pulvirenti, S. Baldazzi, F. Barbano, E. Brattich, S. Di Sabatino, Numerical simulation of air pollution mitigation by means of photocatalytic coatings in real world street canyons, Build. Environ. 186 (2020) 107348, https://doi.org/10.1016/j.buildenv.2020.107348.

[74] M. Rexeis, S. Hausbserger, Trend of vehicle emission levels until 2020-Prognosis based on current vehicle measurements and future emission legislation, Atmos. Environ. 43 (2009) 4689–4698, https://doi.org/10.1016/j.atmosenv.2008.09.034.

[75] J. Richmond-Bryant, R.C. Owen, S. Graham, M. Snyder, S. McDow, M. Oakes, S. Kimbrough, Estimation of on-road NO_2 concentrations, NO_2/NO_x ratios, and related roadway gradients from near-road monitoring data, Air Quality, Atmosphere and Health 10 (5) (2017) 611–625, https://doi.org/10.1007/s11869-016-0455-7.

[76] P. Salizzoni, L. Soulhac, P. Mejean, Street canyon ventilation and atmospheric turbulence, Atmos. Environ. 43 (32) (2009) 5056–5067, https://doi.org/10.1016/j.atmosenv.2009.06.045.

[77] P.W. Seakins, D.I. Langsley, A. Hodgson, N. Huntley, F. Pope, Mobile laboratory reveals new issues -in urban air quality, Atmos. Environ. 36 (2002) 1247–1248, https://doi.org/10.1016/S1352-2310(01)00584-2.

[78] J.H. Seinfeld, S.N. Pandis, in: Atmospheric Chemistry and Physics. From Air Pollution to Climate Change, second ed., John Wiley and Sons, Inc., 2006, ISBN 978-0-471-72017-1, p. 1248.

[79] Z. Šidàk, Rectangular confidence region for the means of multivariate normal distributions, J. Am. Stat. Assoc. 62 (1967) 626–633, https://doi.org/10.2307/2283989.

[80] M. Sperber, Diffuse Lung Disorders: a Comprehensive Clinical-Radiological Overview, Springer Science & Business Media, 2012, ISBN 978-1-4471-3442-8.

[81] A. Strini, S. Cassese, L. Schiavi, Measurement of benzene, toluene, ethylbenzene, and o-xylene gas phase photodegradation by titanium dioxide dispersed in

cementitious materials using a mixed flow reactor, Appl. Catal. B Environ. 61 (2005) 90–97, https://doi.org/10.1016/j.apcatb.2005.04.009.
[82] Tera, In Situ Study of the Air Pollution Mitigating Properties of Photocatalytic Coating, Tera environment, 2009 (Contract number 0941C0978), Report from ADEME and Rhone-Alpes region, France, https://www.atmo-auvergnerhonealpes.fr/publications/eco-coating-etude-situ-des-proprietes-purificatrices-de-revetements-photocatalytiques. (Accessed 22 July 2021). Accessed.
[83] UNI (Ente Nazionale Italiano di Unificazione), Ambient Air-Standard Method for the Measurement of the Concentration of Nitrogen Dioxide and Nitrogen Monoxide by Chemiluminescence, 2012.
[84] S. Vardoulakis, B.E.A. Fisher, K. Pericleous, N. Gonzalez-Flesca, Modelling air quality in street canyons: a review, Atmos. Environ. 37 (2) (2003) 155–182, https://doi.org/10.1016/S1352-2310(02)00857-9.
[85] EMEP, Emissions for 2013, Transboundary Particulate Matter, Photo-Oxidants, Acidifying and Eutrophying Components, EMEP/MSC-W Status Report 1/2015, The Norwegian Meteorological Institute, Oslo, 2015. available online at: https://emep.int/publ/reports/2015/EMEP_Status_Report_1_2015.pdf. (Accessed 24 August 2021).
[86] M. Wegmann, A. Fehrenbach, S. Heinemann, H. Fehrenbach, H. Renz, H. Garn, U. Herz, NO2-induced airway inflammation is associated with progressive airflow limitation and development of emphysema-like lesions in C57bl/6 mice, Exp. Toxicol. Pathol. 56 (6) (2005) 341–350, https://doi.org/10.1016/j.etp.2004.12.004.
[87] M. Weiss, P. Bonnel, J. Kühlwein, A. Provenza, U. Lambrecht, S. Alessandrini, M. Carriero, R. Colombo, F. Forni, G. Lanappe, P. Le Lijour, U. Manfredi, F. Montigny, M. Sculati, Will euro 6 reduce the NOx emissions of new diesel cars? – insights from on-road tests with portable emissions measurement systems (PEMS), Atmos. Environ. 62 (2012) 657–665, https://doi.org/10.1016/j.atmosenv.2012.08.056.
[88] WHO (World Health Organization). https://www.who.int/health-topics/air-pollution#tab=tab_1, 2021. (Accessed 22 July 2021).
[89] X. Xie, C. Hao, Y. Huang, Z. Huang, Influence of TiO2-based photocatalytic coating road on traffic-related NOx pollutants in urban street canyon by CFD modeling, Sci. Total Environ. 724 (2020) 138509, https://doi.org/10.1016/j.scitotenv.2020.138059.
[90] D.S. Wlks, Statistical Methods in the Atmospheric Sciences, 3rd Edition, 100, Academic Press, 2011. ISBN 9780123850225.